Glatiramer acetate reduces infarct volume in diabetic mice with cerebral ischemia and prevents long-term memory loss

Gabrielle Mangin, Marine Poittevin, Christiane Charriaut-Marlangue, Claire Giannesini, Tatiana Merkoulova-Rainon, Nathalie Kubis

Glatiramer acetate reduces infarct volume in diabetic mice with cerebral ischemia and prevents long-term memory loss

Gabrielle Mangin[1], Marine Poittevin[1], Christiane Charriaut-Marlangue[2], Claire Giannesini[3], Tatiana Merkoulova-Rainon[4], Nathalie Kubis[1,5*]

1 Université Paris Diderot, Sorbonne Paris Cité & CART, INSERM U965, F-75475 Paris, France

2 Université Paris Diderot, Sorbonne Paris Cité, INSERM U1141, F-75019 Paris, France

3 Service de Neurologie, AP-HP, Hôpital Saint Antoine, 75012 Paris, France

4 Institut Vaisseaux Sang, Hôpital Lariboisière, Paris, France

5 Service de Physiologie Clinique, AP-HP, Hôpital Lariboisière, 75475 Paris, France

* Corresponding author: Nathalie Kubis, Service de Physiologie and Université Paris Diderot, Sorbonne Paris Cité & CART, INSERM U965, Hôpital Lariboisière, 2 rue Ambroise Paré, 75010 Paris, France. Phone: 33-1-49-95-83-14; Fax: 33-1-49-95-86-71; E-mail address: nathalie.kubis@aphp.fr

Key words: stroke, translational, immunomodulation, inflammation, post-stroke dementia, cognitive decline

ABSTRACT

Stroke is currently the second leading cause of death in industrialized countries and the second cause of dementia after Alzheimer's disease. Diabetes is an independent risk factor for stroke that exacerbates the severity of lesions, disability and cognitive decline. There is increasing evidence that sustained brain inflammation may account for this long-term prejudicial outcome in diabetic patients in particular. We sought to demonstrate that experimental permanent middle cerebral artery occlusion (pMCAo) in the diabetic mouse aggravates stroke, induces cognitive decline, and is associated with exacerbated brain inflammation, and that these effects can be alleviated and/or prevented by the immunomodulator, glatiramer acetate (GA).

Male diabetic C57Bl6 mice (streptozotocin IP) subjected to permanent middle cerebral artery occlusion (pMCAo), were treated by the immunomodulator, GA (Copaxone®) (1mg/kg daily, sc) until 3 or 7 days post stroke. Infarct volume, brain pro- and anti-inflammatory mediators, microglial/macrophage density, and neurogenesis were monitored during the first week post stroke. Neurological sensorimotor deficit, spatial memory and brain deposits of Aβ40 and Aβ42 were assessed until six weeks post stroke.

In diabetic mice with pMCAo, proinflammatory mediators (IL-1β, MCP1, TNFα and CD68) were significantly higher than in non-diabetic mice. In GA-treated mice, the infarct volume was reduced by 30% at D3 and by 40% at D7 post stroke ($P<0.05$), sensorimotor recovery was accelerated as early as D3, and long-term memory loss was prevented. Moreover, proinflammatory mediators significantly decreased between D3 (COX2) and D7 (CD32, TNFα, IL-1β), and neurogenesis was significantly increased at D7. Moreover, GA abrogates the accumulation of insoluble Aβ40.

This work is the first one to evidence that the immunomodulatory drug GA reduces infarct volume and proinflammatory mediators, enhances early neurogenesis, accelerates sensorimotor recovery, and prevents long-term memory loss in diabetic mice with pMCAo.

Highlights:

- GA prevents an increase in proinflammatory mediators after stroke in diabetic mice
- GA reduces infarct volume, accelerates sensorimotor recovery in a diabetic mouse model of stroke
- GA prevents long-term memory loss in a diabetic mouse model of stroke
- GA abrogates the accumulation of insoluble Aβ40 in a diabetic mouse model of stroke

1. Introduction

Ischemic stroke is the second cause of mortality and dementia in industrialized countries and a major health burden (Gorelick et al., 2011). The most important risk factor is hypertension but the pandemic of diabetes announced for 2035 threatens to increase the occurrence of stroke and worsen the already critical situation (Organization). Actually, diabetes increases the risk of stroke and related mortality by three-fold, delays recovery with a more severe residual disability, and increases the risk of post-stroke dementia (Snyder et al., 2015, Chen et al., 2016). Therapeutic strategies are limited and in the acute phase rely on pharmacological (intravenous administration of recombinant tissue plasminogen activator) or mechanical clot removal (Jovin et al., 2015), accessible to less than 10% of patients (Bhaskar et al., 2018). However, patients can still spontaneously improve, mainly within the first three months, suggesting spontaneous plasticity and cortical reorganization in the brain (Kubis, 2016). The immune system is activated early after arterial occlusion and can either aggravate or limit the infarct volume and neurological deficit depending on the timeframe within which it is activated and the cells with which it interacts (Planas et al., 2006). Experimental studies have demonstrated that the time course of microglia/macrophage activation differs according to the stroke model (permanent or transient middle cerebral artery occlusion, pMCAo or tMCAo), and species (Gronberg et al., 2013, Kanazawa et al., 2017). Flow cytometry showed that after transient middle cerebral artery occlusion (tMCAo), this activation occurs as early as 12h in mice (Gelderblom et al., 2009) and at D1 in Wistar rats (Lehmann et al., 2014). In a murine model of tMCAo, the proinflammatory M1 response (considered relatively deleterious) is identified as early as D1 post stroke, remains maximal over the first three days post-arterial occlusion and persists for at least one week (Gelderblom et al., 2009) or two weeks ((Hu et al., 2012), whereas the anti-inflammatory M2 response, (considered relatively beneficial) peaks between D3 and D5, then returns to baseline levels, suggesting a shift to a deleterious profile (Hu et al., 2012).

Basal metabolism in diabetes has been reported to be associated with inflammation. Proinflammatory cytokines (TNFα, IL-β) are increased whereas the anti-inflammatory cytokine IL-10 is decreased in the serum of diabetic patients (Tong et al., 2017). In db/db mice, a genetic model of type 2 diabetes, the proinflammatory cytokines (IL-1β, TNFα, IL-6) are increased in the serum, hypothalamus and hippocampus (Dinel et al., 2011), and similar results are found in rats with type 2 diabetes, with increased IL-1β and INFγ levels in the hippocampus (Hwang et al., 2014). This “basic” inflammation is enhanced in diabetes, and could explain the increased infarct volume, neuronal death and more severe sensorimotor

neurological deficit, at least during the first days post stroke (Dave et al., 2011, Tureyen et al., 2011, Poittevin et al., 2014).

Increased inflammation in diabetics may also play a role in post-stroke dementia that occurs within five years in 25% of stroke survivors. This cognitive decline may be partly due to the toxic effects of the inflammatory CD4+ and CD8+ T cells and B cells accumulating at D14 post stroke in the ipsilateral thalamus (Jones et al., 2018), an area of secondary neurodegeneration that is not initially affected by ischemia but found to degenerate in the months following arterial occlusion (Zhang et al., 2012, Jones et al., 2018). Indeed, beta amyloid peptide (Aβ), a hallmark of Alzheimer's disease where it accumulates in the form of plaques and plays a role in neurotoxicity (Roychaudhuri et al., 2009), has been found to aggregate in the rodent thalamus after tMCAo (van Groen et al., 2005, Makinen et al., 2008), and likely exacerbates the loss of neurons. However, the relationship with post-stroke dementia is unclear and other structures such as the hippocampus, the degeneration of which affects memory loss, have not been investigated in diabetics. Manipulating the immune system to modify the course of post-stroke cognitive decline may be particularly relevant in diabetes, where sustained long-term inflammation likely contributes to a more severe post-stroke neurological and cognitive deficit. In a model of type 1 diabetic mice subjected to pMCAO, we first showed that inflammation was exacerbated in the brain, and that these mice had impaired learning, long-term retention and capacity to learn a new task. We therefore examined the impact of immunomodulation provided by Glatiramer acetate (GA), a disease modifying drug licensed for use in multiple sclerosis that is a demyelinating disease of the central nervous system caused by a Th1-driven excessive proinflammatory response. Although the mechanism of action of GA is has not been clearly elucidated, it is thought to inhibit Th1, promote Th2/Treg responses or reduce microglia/macrophage activation.

2. Materials and methods

All experiments and surgical procedures were performed according to the European Community Directive (2010/63/EU), the ARRIVE (Animal Research Reporting In Vivo Experiments) guidelines, and the French national guidelines for the care and use of laboratory animals. The study was approved by the French ministry of Higher Education for Research and Innovation (#13542-2018051110193197).

2.1. Experimental design

The brain inflammatory profile was assessed in a first set of non-diabetic and diabetic mice at D1 and D7 after induction of cerebral ischemia by permanent middle cerebral artery occlusion (pMCAo).

In a separate set of mice, diabetic mice were subjected to pMCAo at D0 then randomly assigned to daily subcutaneous saline solution (vehicle) or GA for 3 days or 7 days. Sensorimotor examination was conducted at D1, D3, D7 and D14, and cognitive function was assessed at weeks 5 and 6 (between D29 and D40) after induction of cerebral ischemia. Infarct volume, microglia/macrophage, T lymphocytes and neurogenesis density analyses were performed at D3 and D7. Quantification of inflammatory and immune markers (COX2, CD32, TNFα, CD86, IL-1β and CD206, Arg1, IL-4, TGFβ, IL-10) in the brain at D3 and D7 and in the blood (TNFα, IL1β, INFγ, IL4 and IL10) at D3 and D40. Soluble and insoluble fractions of Aβ40 and Aβ42 D40 were quantified in the brain at D40 (Supplementary Figure 1). We have previously shown that diabetic mice subjected to pMCAo had an increased infarct volume and worsened neurological deficit compared to non-diabetic mice (Poittevin et al., 2015). Infarct volume in non-diabetic mice subjected to pMCAO and treated with GA, was no different to that of vehicle-treated mice (Poittevin et al., 2013). Lastly, in a preliminary study, we sought to identify whether post-stroke cognitive decline occurred only in diabetic mice subjected to pMCAO and not in non-diabetic mice subjected to pMCAo. For these three reasons, we only assessed the efficacy of GA in diabetic mice subjected to pMCAo. As control groups for the assessment of cognitive decline, sham non-diabetic mice (C), sham diabetic mice (D), and non-diabetic mice subjected to pMCAO were also evaluated. All experiments were conducted by investigators blinded to the status (diabetic and non-diabetic) and the treatment (GA or saline solution).

2.2. Diabetes induction

Male C57BL/6J mice (Janvier, Le Genest Saint-Isle, France) were housed in a 12h light-dark cycle and had free access to food and water. At the age of six weeks, with a mean body weight of 20g, mice were divided into two groups: one group received five consecutive daily intraperitoneal (IP) injections of STZ (60 mg/kg in 100 µL of citrate buffer) to induce diabetes, and the other a sham injection of the vehicle (citrate buffer). Glycemia was tested weekly for 8 weeks. Mice with sustained hyperglycemia (>300 mg/dL) were considered as diabetic (90% of treated mice).

2.3. Permanent Middle Cerebral Artery occlusion (pMCAo)

Mice were anesthetized with isoflurane (initially 2%, followed by 1.5 to 1.8% in O_2) and body temperature was continuously monitored to ensure it remained at 37 ± 0.5°C using a heating blanket (Homeothermic Blanket Control Unit; Harvard Apparatus Limited, UK). They were subjected to permanent focal cerebral ischemia by electrocoagulation of the middle cerebral artery as described previously (Poittevin et al., 2013). D0 refers to the day of pMCAo.

2.4. Drug treatment

Each animal received a subcutaneous injection of either 200µL saline solution (vehicle) or 2mg glatiramer acetate (GA) (Copaxone®) (Sanofi, Paris, France) in 200µL saline solution for three or seven consecutive days, immediately after the end of surgery, approximately 5 minutes after occlusion of the MCA.

2.5. Sensorimotor deficit assessment

At D-1, all mice underwent a one-day training phase in order to avoid biases linked to learning and stress. At D1, D3, D7 and D14 after pMCAo, the mice selected for the long-term study underwent a neurological evaluation consisting of five tests: neurological score, grip and string test, beam walking and pole test. The maximum global score was 19, with the lower neurologic score corresponding to a more severe deficit (Haddad et al., 2008).

2.6. Cognitive assessment

Before testing spatial memory (Barnes Maze) in mice at D40, we verified that there was no persistent sensorimotor deficit by determining the global neurological score at D14, and assessing spontaneous locomotor activity (open field) at D27 and D28. At D29, mice were placed in the "behavior" room so they could become accustomed to the environment where they were subjected to a 12h night-day cycle with food and water provided ad libitum.

2.6.1. Open field

Spontaneous locomotor activity was evaluated in the open field to detect any residual sensorimotor deficit or potential anxiety likely to cause the mice to "freeze", thus skewing the results of the Barnes Maze test. The open field is a chamber (50×50×40 cm) made of light gray polyvinylchloride (TSE systems GmbH, Bad Homburg, Germany) from which the mice cannot escape. The open field is fitted with a top-mounted charge-coupled infrared video camera and lit by diffuse white light (5 Lux). Spontaneous activity (total distance traveled in cm and mean velocity in cm/s) was measured automatically for 30 minutes by an EthoVision

XT system and analyzed by EthoVision XT 11.5 tracking software (Noldus, Wageningen, The Netherlands). Open field activity was assessed at D27 and D28 in four groups: vehicle, GA, diabetic mice without stroke (D)—to check whether diabetes alone was sufficient to affect the test—and control mice (C) (no diabetes and no stroke).

2.6.2. Barnes Maze

The Barnes Maze tests the ability of a mouse placed in the maze, to learn and remember the location of an escape box using visual clues around the testing area. As previously described (Cifuentes et al., 2017), the maze is an open space one meter in diameter; it is painted white and brightly lit to create an anxiety-provoking environment. There are 20 holes spaced equidistantly around the circumference. A black escape box is randomly placed under one of these holes that the mouse will seek for shelter. The mouse is placed into an opaque white cylinder in the center of the maze for 10 seconds to disorientate it. The cylinder is then removed and the mouse is allowed to explore the maze. Mice are trained three times a day with a 15-minute rest between each trial. The location of the escape box is randomly assigned and changes between mice. For the first four days, in the training phase, the mouse has to learn the location of the escape box hidden beneath one of the 20 holes. Learning is measured by the gradually shorter time spent before finding the escape box. After a two-day break, during which the mice are left undisturbed in their home cage, they are once again placed in the Barnes Maze to measure their ability to recall the location of the escape box in the retention phase (7^{th} day of evaluation). One day later, the escape box is changed to a different location, and during that phase (reversal phase) that lasts 3 days (8^{th}, 9^{th} and 10^{th} days of evaluation), the mice's ability to learn and retain a new location is measured.

The Barnes Maze test was conducted one month after induction of cerebral ischemia, between D29 and D39. The behavior of mice in the maze during each phase was recorded with the camera, and the time required to find the escape box (latency to escape) was measured.

2.7. Assessment of infarct volume and edema

On the day of sacrifice (D3 or D7), mice were transcardially perfused with heparinized saline, followed by 4% paraformaldehyde (PFA) in 0.1 M phosphate buffer, pH 7.4. Brains were removed, post-fixed overnight in PFA and cryoprotected in 20% sucrose. Coronal 30 µm-thick sections were cut frozen using a cryostat CM 1950 (Leica Biosystems, Nussloch, Germany). Every eighth 30µm-thick floating section was stained with Cresyl violet. The cortical infarct area was measured using ImageJ software (National Institutes of Health,

Bethesda, MD), to calculate the stroke volume (mm^3) by integrating measured areas and distances between sections. Measured infarct volume was corrected for edema with the following formula: corrected infarct volume = measured infarct volume x (contralateral hemisphere volume/ipsilateral hemisphere volume) as already described (Poittevin et al., 2013).

2.8. Immunohistochemistry

30µm-thick floating coronal sections were incubated with primary antibody overnight at 4°C—anti-Ki67 (1:200, Abcam, Cambridge, UK), anti-doublecortin (DCX) (1:100, Santa Cruz, Dallas, TX), anti-Iba1 (1:200, Wako, Japan), anti-CD3 (1:200, Dako, Santa Clara, USA) and anti-glucose transporter-1 (Glut-1) (1:500, Millipore, Burlington, MA) to detect proliferative cells, neuroblasts, microglia/macrophage cells, T cells and vessels, respectively. Appropriate fluorescent-labelled secondary alexa fluor 594 or 488 antibodies (Molecular Probes, Eugene, OR, 1:400) were applied for one hour at room temperature. Specificity was checked by omitting the primary antibody.

2.9. Morphological analysis

Counting was conducted blind with respect to mouse status on three coronal brain sections at +0.80 mm, -0.80 mm, and -1.20 mm relative to bregma, all of which consistently included the infarct area.

Cell proliferation (D3) counting was assessed in the ipsilateral hemisphere including the subventricular zone (SVZ) in particular, and expressed by the average number of Ki67+ cells/section.

Neurogenesis (D7) counting was assessed as described for cell proliferation and expressed as the average number of Ki67+/DCX+ cells/section.

Microglial/macrophage cell density was manually evaluated in three randomly chosen regions of interest (ROI, 0.15 mm^2) in the peri-infarct area by counting Iba1+ cells with an amoeboid aspect at D3. Because cell density increased dramatically at D7, individual cell-count was impossible. Microglial/macrophage cell density was therefore assessed by calculating the Iba1+-positive area using NIH ImageJ software (10X) (arbitrary units). To account for the varying infarct volumes between groups, microglia/macrophage density was further expressed as the following ratio: cell density/infarct volume (number of cells/ROI/mm^3).

T-cell density was manually assessed in the whole section by counting CD3+ cells at D3 and D7.

2.10. RT-PCR analysis

RNAs were isolated from the ipsilateral brain hemisphere using the RNEasy lipid tissue mini kit (Qiagen, Courtaboeuf, France). Reverse transcription was performed with Ready-to-Go RT-PCR Beads (GE Healthcare, Uppsala, Sweden) and real-time PCR with FS Essential DNA Green Master (Roche, France) on a LightCycler from Roche. The primers used for PCR are listed in Table 1. The primer set specific for mouse peptidylprolyl isomerase A (cyclophilin A) was purchased from Qiagen. All assays were performed in triplicate. The mRNA levels were normalized to the cyclophilin A mRNA content.

2.11. Multiplex analysis

Blood proteins were analyzed using multiplex technology on a MAGPIX system (MILLIPLEX® Analyst 5.1 software) as recommended by the manufacturer. The panel (Bio-Techne, UK) included TNFα, IL1β, INFγ, IL4 and IL10.

2.12. Aβ40 and Aβ42 quantification

At D40 post stroke, mice were perfused with heparinized saline, brains were rapidly removed, snap frozen in liquid nitrogen and stored at -80°C. Brain hemispheres were homogenized at 10% (w/v) in phosphate buffered saline (PBS) containing protease inhibitor cocktail 2 Sigma-Aldrich (St Lois, MO) using a MagNA Lyser homogenizer (Roche, Rotkreuz, Switzerland), 2 x 25 sec at 6500 rpm. One half of each homogenate was centrifuged at 25,000 x g for 60 minutes at 4°C, the supernatants were collected (soluble fraction), and the protein concentration in the supernatants was determined using the BCA Protein Assay Reagent (Pierce, Rockford, IL). The other half of the homogenate was added to 8x mass of cold 5 mol/L guanidine-HCl containing 50 mmol/L trisHCl, pH 8.0, homogenized thoroughly using an Ultra Turrax T25 homogenizer, and incubated at room temperature for 4 hours with rotation. The homogenates were then diluted with cold Dulbecco's phosphate-buffered saline containing 5% BSA, 0.03% Tween-20 and protease inhibitor cocktail 2 (Sigma-Aldrich) at 1:20, and centrifuged at 16,000 × g for 20 minutes at 4°C (insoluble fraction). Millipore's MILLIPLEX MAP Human Neurodegenerative Disease Magnetic Bead Panel 4 kit (Merck KGaA, Darmstadt, Germany) was used for simultaneous quantification of Aβ40 and Aβ42 peptides in both soluble and insoluble fractions of the brain, according to the manufacturer's

instructions. The results were read on a MAGPIX instrument (Luminex Corporation, Austin, TX) and analyzed using the χPONENT for MAGPIX 4.2 software (Luminex).

2.12. Statistical analysis

Statistical analyses were performed with Prism 7.02 software (GraphPad, San Diego, CA). Data are expressed as mean±SD. The Shapiro-Wilk normality test was used to assess whether the data were consistent with a Gaussian distribution. Comparisons between GA and vehicle groups were made using a *t*-test or a non-parametric Mann-Whitney at each time point. Two-way ANOVA for repeated measures was used to analyze data in the training (1st–4th days) and reversal (8th –10th days) phases in the Barnes Maze test. Post-hoc analyses were performed using Bonferroni's multiple comparison tests. A value of $P<0.05$ was considered statistically significant.

3. Results

Before surgery, 30% of mortality was due to diabetes. At D0, there was no significant difference in mean glycemia between the vehicle-treated mice and the GA-treated mice (425.00±69.60 and 442.40±70.79, respectively). In the GA group, two mice died at D3 and three at D7, and in the Vehicle group, one died at D3 and two at D7. At D40, two GA mice died versus six in the Vehicle group. Glycemia levels were not significantly different between the vehicle-treated mice and the GA-treated mice prior to treatment allocation (452,90±63,40 and 442,40±70,79 mg/dl, $P = 0.67$, respectively), or after 7 days of daily GA injections (499,60±66,74 and 453,00±68,62 mg/dl, $P = 0.22$, respectively).

3.1. GA improves sensorimotor deficit in diabetic mice at D3

At D1, compared to D-1, we observed a significant reduction in the neurological score in both the GA- (13.75±3.61, n=20 versus 17.80±1.20, n=20, respectively; $P <0.0001$) and Vehicle-treated mice (12.47±3.70, n=19 versus 18.05±1.35, n=19, respectively; $P <0.0001$) (Figure 1). There were no significant differences between the two treated groups at D1, indicating that the surgery induced a similar neurological deficit that remained unchanged 24 hours after administration of GA. At D3, the scores were significantly higher in GA mice compared to Vehicle mice (13.60±1.64, n=20 versus 10.63±3.61, n=19; $P = 0.002$) indicating a quicker recovery in the GA-treated mice. However, no further differences were found between the two groups at D7 (14.45±2.78, n=20 versus Vehicle 12.95±4.37, n=19; $P = 0.21$) and at D14 (17. 19±1.47, n=16 versus 16.63±1.67, n=16; $P = 0.32$) (Figure 1).

At D7, compared to D3, there was no significant change in the neurological score in either the Vehicle- ($P = 0.083$) or the GA-treated mice ($P = 0.25$). At D14, compared to D-1, GA mice ($P = 0.18$) had normalized neurological scores whereas evidence of sensorimotor impairment was still present in Vehicle-treated mice ($P = 0.0018$); this however was normalized before the open field and Barnes Maze assessments.

3.2. GA improves the retention task in diabetic mice

3.2.1. Open field

In order to avoid interpretation biases, we first verified the ability of mice to spontaneously walk the equivalent distance with similar velocity in an open field. We compared control mice (C), diabetic mice without pMCAo (D), non-diabetic mice with pMCAo (pMCAo), diabetic mice with pMCAo treated with saline solution (Vehicle) and diabetic mice with pMCAo treated with GA (GA) (Figure 2A). Overall ANOVA of these data showed that there was a significant difference between the five groups in the total distance travelled spontaneously by the mice in the open field ($P = 0.0015$). Post-hoc analysis showed no significant differences between GA, Vehicle, D or pMCAo mice in terms of the total distance travelled (7131±1328cm, n=15 versus 6803±1341cm, n=15 versus 6086±1627cm, n=8 versus 7573±1674cm, n=10, respectively). However, compared to the control group (9542±1554cm, n=10), the distance travelled by mice in all three diabetic groups was significantly less (C vs D, $P < 0.001$; C vs Vehicle, $P < 0.01$, C vs GA, $P < 0.05$). The distance travelled by pMCAo mice was not significantly different from that of control mice. Likewise, although mean velocity did not differ between the three diabetic groups, it was significantly lower compared to controls (GA 4.21±0.79cm/s, n=15; Vehicle 3.96±0.74cm/s, n=15 and D 3.38±0.90cm/s, n=8) versus (C 5.30±0.86cm/s, n=10) whereas the difference in mean velocity between pMCAo mice (4.33±0.75cm/s n=10) and control mice was not statistically significant, with an overall significance of $P = 0.0015$ (Figure 2A).

3.2.2. Barnes Maze (Table 2)

In the training phase, two-way repeated measures ANOVA showed a significant reduction in the latency to escape between the 1st day and the 4th day (n=7-17, $P < 0.0001$) in all five groups (Figure 2B). Post-hoc analysis showed no significant differences over time between the five groups (GA, Vehicle, pMCAo, D, and C) in terms of their learning ability to find the escape box, except in GA mice at D3 that showed a significantly increased latency compared

to pMCAo mice ($P < 0.05$). No significant differences were found between any groups on the 4th day. All five groups accomplished the training phase with similar efficacy indicating that GA did not accelerate the learning process.

After two days of rest, the overall one-way ANOVA in the retention phase showed a significant difference between the groups (n=7-17, $P < 0.0001$). Latency to escape was increased in Vehicle mice compared to GA mice ($P < 0.001$), D mice ($P < 0.01$), C mice ($P < 0.05$), and non-diabetic pMCAo mice ($P < 0.001$) indicating that pMCAo induced a significant impairment in diabetic mice and that GA significantly improved the long-term spatial memory in these mice (Figure 2B).

In the reversal phase, there was an overall significant reduction in the latency to escape between the 8th day and the 10th day (n=7-17, $P < 0.0001$). Post-hoc analysis showed that at the beginning of the reversal phase (8th day after starting the Barnes Maze evaluation), Vehicle mice showed a significantly increased latency to escape compared to control mice ($P < 0.0001$), D mice ($P < 0.01$) and pMCAo mice ($P < 0.0001$); GA-treated mice performed less well than the C mice ($P < 0.05$). No significant differences were found in other pairwise comparisons (Figure 2B). On the 9th and 10th days of evaluation, a significantly increased latency to escape persisted in Vehicle mice compared to control mice ($P < 0.01$ and $P < 0.05$, respectively), to diabetic mice ($P < 0.01$ and $P <0.05$, respectively), and to pMCAo mice ($P < 0.001$ and $P <0.01$, respectively). Moreover, on the 9th day, a significant difference was found between our GA and Vehicle groups ($P < 0.01$), suggesting that GA mice were able to recall the new information whereas this was not the case for Vehicle mice at any time of the reversal phase. No more significant differences were detected between GA mice and any of the other four groups, at the other stages of the evaluation (Figure 2B).

To summarize, Vehicle mice (diabetic mice with pMCAo) showed cognitive impairment that was reflected in the increased latency to find the escape box in the retention phase and in the reversal phase (8th, 9th and 10th days) of the Barnes maze test, compared to C, D and pMCAo mice. In the retention phase, GA averted the long-term spatial memory deficiency that was evidenced in diabetic mice after pMCAo. In the reversal phase, there was a significantly lower latency to escape in the GA mice compared to the Vehicle mice on the 9th day, indicating an improvement in treated mice.

3.3. Stroke volume and edema

At D3, infarct volume was significantly reduced in GA mice compared to Vehicle mice (11.78±1.60mm^3, n=7 versus 15.17±2.77mm^3, n=7, respectively; $P = 0.016$) (Figure 3). This

difference persisted at D7 and was even greater (2.59±1.28mm^3, n=7 versus 7.08±3.73mm^3, n=7, respectively; P = 0.011). No hemorrhage was observed during brain extraction or during preparation of coronal sections. No significant differences in terms of edema volume were observed between the two groups at D3 (1.50±1.42, n=7 vs 3.10±3.48, n=7, respectively; P = 0.28) (Figure 3).

3.4. Microglia/macrophage and T-cell density

Microglia/macrophage cells (Iba1+) adopted a round amoeboid shape in the peri-infarct area at D3 and D7, indicating a change in the state of activation. At D3, no differences in microglia/macrophage cell density were evidenced between GA and Vehicle mice (51.00±12.81 cells/ROI, n=7 versus 50.71±8.16 cells/ROI, n=7, respectively; P = 0.96), nor at D7 (0.26±0.69 a.u./section, n=7 versus 0.30±0.11 a.u./section, n=7, respectively; P = 0.17) (Figure 4).

T cells predominated in the peri-infarct area, were scarce at D3 and D7 but dramatically increased by D40 and densely packed in the peri-infarct area. No differences in T cell density were evidenced between GA and Vehicle mice at D3 (30.9±16.5 cells/section versus 31.1±27.2 cells/section, respectively; P = 0.65) or at D7 (33.0±22.4 cells/section versus 28.4±7.5 cells/section, respectively; P = 0.60) (n=6-7).

3.5. RT-PCR analyses of the expression of inflammatory mediators

3.5.1. Diabetes induces up-regulation of brain mRNA encoding for proinflammatory cytokines in mice subjected to pMCAo

At D1 post stroke, diabetic mice had increased expression of IL-1β (P = 0.025), MCP1 (P = 0.038), IL-6 (P = 0.00076) and TNFα (P = 0.0032) mRNA compared to non-diabetic mice, whereas CD68 and IL-4 mRNA levels were not significantly different between groups (Table 3).

At D7 post stroke, diabetic mice showed increased expression of IL-1β (P = 0.0032), MCP1 (P = 0.05), TNFα (P = 0.0025) and CD 68 (P = 0.027) mRNA but also down-regulation of the anti-inflammatory cytokine IL-4 mRNA (P = 0.0023) whereas IL-6 mRNA levels were not significantly different compared to non-diabetic mice (Table 3).

3.5.2. Proinflammatory mediator expression is reduced in the brain of GA mice as early as D3 and at D7

At D3, **COX2** mRNA was significantly decreased in GA mice compared to Vehicle mice (0.40±0.14 a.u., n=7, versus 2.74±3.01 a.u., n=8; $P = 0.014$). **CD32** mRNA expression was not impacted by GA treatment (0.77±0.25 a.u., n=8, versus 1.13±0.42 a.u., n=8; $P = 0.059$), nor was **TNFα** mRNA expression (2.18±1.35 a.u., n=8 versus 2.93±2.40 a.u., n=8; $P = 0.45$), **CD86** (0.51±0.17 a.u., n=8, versus 0.64±0.42 a.u., n=8, $P = 0.45$) or **IL-1β** (0.32±0.67 a.u., n=6 versus 0.06±0.03 a.u., n=7; $P = 0.80$) (Figure 5A).

At D7, **COX2** mRNA levels were not significantly different between GA and Vehicle mice (0.41±0.11 a.u., n=7 versus 0.53±0.44 a.u., n=7; $P = 0.74$), whereas **CD32** mRNA remained significantly decreased (0.05±0.45 a.u., n=6, versus 0.51±0.45 a.u., n=7, $P = 0.014$). **TNFα** mRNA was dramatically decreased (0.06±0.03 a.u., n=7 versus 36.72±25.71 a.u., n=7) ($P = 0.0006$). **CD86** mRNA levels were not significantly different between the groups (1.23±0.11 a.u., n=7 versus 1.12±0.29 a.u., n=7; $P = 0.45$). **IL-1β** mRNA was significantly decreased (0.18±0.082 a.u., n=6 versus 37.76±41.44 a.u., n=7; $P = 0.035$) (Figure 5B).

Between D3 and D7, **COX2** mRNA expression did not change significantly in GA mice ($P = 0.80$), whereas in Vehicle mice, COX2 mRNA levels decreased significantly at D7 ($P = 0.029$). **CD32** mRNA expression decreased significantly from D3 to D7 in GA mice ($P = 0.0007$) and in Vehicle mice over time ($P = 0.017$). **TNFα** mRNA expression decreased significantly in GA mice ($P = 0.00030$), whereas it increased in Vehicle mice ($P = 0.0031$). **CD86** expression increased in GA mice ($P = 0.00030$) and in Vehicle mice ($P = 0.021$), as did **IL-1β** ($P = 0.0012$ and $P = 0.0072$, respectively) (Supplementary Figure 2).

To summarize, administration of GA strongly reduced the expression of proinflammatory mediators as early as D3 (COX2) and at D7 (CD32, TNFα and IL-1β). CD86 expression was not affected by GA at either of these two time points in our model.

3.5.3. Anti-inflammatory mediator expression is not modified in the brain by GA at D3 but later, at D7

At D3, **CD206** mRNA levels were not significantly different between GA and Vehicle mice (1.19±0.47 a.u., n=8 versus 1.49±0.96 a.u., n=8, $P = 0.45$), nor were **Arg1** mRNA (0.72±0.30 a.u., n=8 versus 1.48±1.26 a.u., n=8; $P = 0.38$), **IL-4** mRNA (2.43±2.87 a.u., n=6 versus 2.04±1.93 a.u., n=5; $P > 0.99$), **TGFβ** mRNA (0.87±0.39 a.u., n=8 versus 1.20±0.57 a.u., n=8; $P = 0.19$) or **IL-10** mRNA levels (2.07±1.80 a.u., n=6 versus 3.04±2.42 a.u., n=7; $P = 0.43$) (Figure 6A).

At D7, **CD206** expression was not significantly different between GA and Vehicle mice (1.25±0.25 a.u., n=5 versus 1.52±1.01 a.u., n=7; *P* = 0.83), nor was **Arg1** (0.065±0.0.60 a.u., n=5 versus 0.050±0.035 a.u., n=7, *P* = 0.90), **TGFβ** expression (0.84±0.59 a.u., n=5 versus 1.90±1.48 a.u., n=7; *P* = 0.19) or **IL-10** (0.71±0.19 a.u., n=5 versus 057±0.17 a.u., n=6; *P* = 0,33). **IL-4** was however significantly increased in GA-treated mice (0.92±0.50 a.u, n=5 versus 0.099±0.074 a.u., n=7; *P* = 0.0025) (Figure 6B).

Between D3 and D7, there were no significant changes in the levels of expression of **CD206** mRNA in GA mice (*P* = 0.23) or in Vehicle mice (*P* = 0.95). **Arg 1** mRNA decreased drastically and significantly between D3 and D7 in both GA mice (*P* = 0.0021) and Vehicle mice (*P* = 0.0014). **IL-4** expression levels decreased dramatically in both groups, although to a lesser extent in GA mice (*P* = 0.0087) than in Vehicle mice (*P* = 0.0012). **TGFβ** mRNA expression levels did not change significantly in GA mice (*P* = 0.96) or Vehicle mice (*P* = 0.69). **IL-10** mRNA levels decreased between D3 and D7 in Vehicle mice (*P* = 0.022) but not in GA mice (*P* = 0.33) (Supplementary Figure 3).

To summarize, administration of GA did not modify anti-inflammatory mediator expression at D3 but strongly increased the expression of IL-4 by D7 in our model.

3.6. Systemic inflammation is not modified by GA at D3 or D40

Protein quantification of pro- (IL1β, TNFα, INFγ) and anti-inflammatory (IL4, IL10) cytokines was performed at D3 and at the end of the cognitive assessment procedure (week6/D40) in the blood. We found no significant differences between GA and Vehicle mice (n=6-7) (Table 4).

3.7. Neurogenesis increased in GA-treated mice

As evidenced by Ki67 immunostaining at D3, there were no differences in cell proliferation between GA mice (93.45±22.87 cells/ipsilateral section, n=5) and Vehicle mice (83.80±35.40 cells/ipsilateral section, n=5; *P* = 0.80). At D7, proliferation was greater but remained at similar levels in both groups. However, double immunostaining at D7 with anti-Ki67 and anti-DCX antibodies to identify proliferating neuroblasts showed significantly more double-stained cells in GA mice compared to Vehicle mice (101.00±14.80 Ki67-DCX cells/ipsilateral section, n=7 versus 78.50±10.93 Ki67-DCX cells/section, n=5; *P* = 0.028) suggesting that neurogenesis was favored by GA. These neuroblasts migrated from the subventricular zone to the peri-infarct area but none were found in the hippocampus (Figure 7).

3.8. Aggregated Aβ40 accumulation is prevented by GA treatment

In order to establish whether the generation and/or deposition of neurotoxic amyloid beta was modulated by GA in diabetic mice after pMCAo, we used a multiplex immunoassay to detect Aβ42 and Aβ40 peptides in soluble and insoluble fractions of the brain homogenates. We found that at six weeks post stroke, Aβ42 peptide was present in the soluble fraction of brains from both GA- and Vehicle-treated groups, with no significant inter-group differences in concentration (22.02±6.59 pg/mg of total protein, n=8 and 17.29±3.81 pg/mg of total protein, n=8, respectively; $P = 0.10$). However, no Aβ42 peptide was detected in the insoluble fraction of brains from GA or Vehicle mice, suggesting that Aβ42 did not accumulate and aggregate in diabetic mice after pMCAo. In contrast, Aβ40 was detected in both soluble and insoluble brain fractions. Although Aβ40 increased significantly in the soluble fraction of brains from GA mice compared to Vehicle mice (7.56±6.99 pg/mg of total protein, n=8 versus 1.81±0.48 pg/mg of total protein, n=8; $P = 0.0054$) (Figure 8), considerably higher levels of Aβ40 were found in the insoluble fraction of brains from Vehicle mice (225.70±76.75 pg/ml of total protein) demonstrating increased accumulation and aggregation of Aβ40 in diabetic mice after pMCAo (Figure 8). Remarkably, Aβ40 was undetectable in the insoluble fraction of GA mice, suggesting that GA treatment protected against Aβ40 accumulation and aggregation after pMCAo in diabetic mice.

4. Discussion

We showed that early subcutaneous administration of daily (for one week) GA in diabetic mice subjected to pMCAo accelerated sensorimotor recovery, prevented long-term memory impairment, and reduced the expression of proinflammatory mediators thus reducing infarct volume and increasing neurogenesis.

Ours is the first study to demonstrate the acute and long-term neuroprotective effect of GA in diabetic mice following experimental cerebral ischemia. In a recent meta-analysis of the different immunotherapeutic strategies approved for multiple sclerosis and used in stroke (Dreikorn et al., 2018), only four studies on the use of GA in experimental stroke were reported, including one from our own laboratory (Poittevin et al., 2013). Two of the studies cited did not show a reduction in infarct volume or improvement in neurological outcome after pMCAo (Poittevin et al., 2013) or tMCAo (Kraft et al., 2014) in mice. The other two studies were conducted in rats and showed an improvement in these two parameters (Ibarra et al., 2007, Cruz et al., 2015). GA application (dose, route, and treatment window), read-out times, and intended outcomes differed between the studies. Because a higher dose did not show superior efficacy in mice (Kraft et al., 2014), we decided to use the same dose as in our previous experiments (Poittevin et al., 2013), and which is routinely used in experimental autoimmune encephalomyelitis studies in mice. As the time course of recruitment of different inflammatory mechanisms after stroke is not clearly understood, we opted for daily injections to maximize the chances of GA targeting the appropriate proinflammatory steps and favoring polarization towards the anti-inflammatory phenotype. We limited the treatment period to seven days because we hypothesized that reducing the initial proinflammatory response would be sufficient to prevent post-stroke dementia.

All previously reported experimental studies have focused on sensorimotor evaluation in the acute phase with the exception of one, in which post-stroke outcome was evaluated at 60 days (Cruz et al., 2015); memory function was however not assessed. Our study is the first to examine the effect of GA on cognitive function one month after pMCAo in diabetic mice using the ten-day Barnes Maze test. We showed that spatial memory was unaffected in non-diabetic pMCAo mice, explaining why only diabetic mice received GA in our protocol. We favored the pMCAo stroke model in diabetic mice because we had previously shown that the tMCAo stroke model in diabetic mice was associated with significant mortality after D7. The pMCAo stroke model has also the advantage of being a more representative model of the clinical condition. Indeed, pMCAo mimics the large vessel occlusion that occurs in 88.7–97.5% of ischemic strokes, whereas tMCAo represents only 2.5–11.3% of patients (McBride

and Zhang, 2017). Moreover, pMCAo is considered a more "inflammatory" model than tMCAo (Zhou et al., 2013), which increases activation of microglia and enhances infiltration of circulating leukocytes in the cerebral parenchyma (Liesz et al., 2015). Lastly, we set out to develop a stroke model that "spared" the hippocampus since our hypothesis was that inflammation triggered remote lesions or brain cortical remapping leading to long-term memory deficit.

We established that expression of proinflammatory mediators within the brain was exacerbated in diabetic mice following pMCAo compared to non-diabetic mice. This occurred as early as D1, through upregulation of IL-1β, MCP1, IL-6, TNFα that persisted at D7 - although to a lesser extent for IL-6 - and downregulation of the anti-inflammatory TGFβ cytokine at D1 only. Together, these results may explain the discrepancy between our previous (Poittevin et al., 2013) and the present findings on the therapeutic efficacy of GA in a mouse model of pMCAo. The greater impact of GA in pMCAo diabetic mice compared to pMCAo non-diabetic mice (Poittevin et al., 2013) may be related to this increased inflammation that could likely be modulated by treatment. In non-diabetic mice, the level of inflammation was too low to be measured or to serve as a useful target for therapeutic intervention, or not notably modified by the single injection of GA that we used in our first protocol.

After induction of stroke, both microglia, which reside in the CNS, and monocytes, which infiltrate the brain, play major roles in the acute phase of inflammation. They display a range of functional states, depicted by morphological changes, specific surface antigen expression and production of molecules in response to environmental cues. Common characteristics include phenotypic markers, such as Iba1 or CD11b, the ability to polarize from a classic proinflammatory M1 to an alternative anti-inflammatory and pro-healing M2 phenotype with various states of activation (M2a, M2b, M2c, M2d) characterized by a set of markers (Franco and Fernandez-Suarez, 2015). Activation is driven by the danger-associated molecular patterns released by dying neurons (Fumagalli et al., 2015), leading the microglia/macrophages to a phagocytic activity that may be cytotoxic through killing cells or protective through scavenging debris. Once activated, microglial cells adopt a round amoeboid shape that is indistinguishable from macrophages that are both recognized by the Iba1 antibody. In our study, Iba+ cell density was not significantly different between groups and across time. To distinguish between the different states of inflammation, we characterized the proinflammatory M1 phenotype by the polarization markers CD32 and CD86 associated with increased IL-1, TNFα and COX 2 (Chhor et al., 2013), and the alternative anti-

inflammatory M2 phenotype through CD206 and arginase 1, associated with increased IL-4, IL-10 and TGFβ (Benakis et al., 2014, Fumagalli et al., 2015). We showed that some of the associated proinflammatory M1 markers were down-regulated by GA at D3 (COX 2), and at D7 (CD32, IL-1β and TNFα), whereas anti-inflammatory markers were not significantly modified, except for IL-4 that was increased at D7 by GA, suggesting that in our experimental model, GA was mostly effective on the M1 cell phenotype. As IL-4 is also secreted by Th2 cells (Stein et al., 1992), we cannot exclude a possible associated participation of LT, even though we did not observe any differences in T lymphocyte density between groups. Nor can we exclude the involvement of pericytes, which can adopt a microglial-like phenotype after ischemia by expressing microglial markers such as Iba1, CD11b, GAL-3, TNFα and MHCII (Ozen et al., 2014), though this requires further investigation. In the blood, we could not evidence any differences between treated and untreated groups in main pro-and anti-inflammatory cytokines (TNFα, IL1β, INFγ, IL4 and IL10) either at D3 or at D40. Understanding the mechanisms through which GA is effective is fundamental. This still remains to be completely understood in the context of multiple sclerosis as well, and deserves to be investigated specifically in a new study, with a particular focus on the "brain and systemic inflammatory relationships", including liver, spleen and bone marrow.

At D3, we found that cerebral ischemia induced proliferation of the cells located in the SVZ of the ischemic hemisphere that was not significantly different between GA mice and Vehicle mice. At D7, GA significantly increased the number of proliferating neuroblasts, the majority of which were found in the SVZ and the corpus callosum but had still not reached the border of the infarct. We postulate that the reduced expression of proinflammatory cytokines favored a less deleterious environment in the brain of GA-treated mice, and enhanced neurogenesis. Indeed, in a "favorable environment" such as in the presence of anti-inflammatory cytokines secreted by Treg (IL-10 and TGFβ) and Th2 (IL-4), microglia trigger the proliferation of neuronal progenitors *in vitro*, whereas proinflammatory Th1 cytokines (TNFα and IFNγ) block neurogenesis (Ekdahl et al., 2009). In our previous study of non-diabetic mice subjected to pMCAo or tMCAo, we also observed significantly greater neurogenesis in GA-treated mice subjected to pMCAo only, but we were unable to demonstrate the impact of GA on the proinflammatory environment (Poittevin et al., 2013). This may have been due to the lower basic inflammatory status in the absence of diabetes.

Spatial memory, used in spatial navigation in unknown places, involves working memory, and short- and long-term memory, and is impaired in post-stroke patients (Srikanth et al., 2003).

Spatial memory forms in specific areas of the brain, including the hippocampus (Burgess et al., 2002). The Barnes Maze test, which relies on hippocampal-dependent spatial reference memory (Harrison et al., 2009), seems to be the most appropriate test given that inflammation is particularly exacerbated in that region in mice with hyperglycemia (Dinel et al., 2011); it is also less anxiogenic than the Morris water maze. Mice are not natural swimmers and perform less well than rats in the Morris water maze (Whishaw, 1995). The Barnes Maze also offers a more complex assessment than the T- or Y-Maze. In the open field, the distance traveled and mean velocity were impaired to the same extent in the 3 groups of diabetic mice (Diabetic, Vehicle and GA) and we can only speculate on that result: anxiety, fatigability or subtle locomotor impairment likely induced by the hyperglycemia. However, the Barnes Maze—which evaluates memory through locomotor activity—clearly showed that the only difference between the 5 groups was that the diabetic mice subjected to pMCAO without GA (Vehicle mice) performed less well than the other groups, and in particular less well than the diabetic mice subjected to pMCAO treated with GA, indicating that diabetes *per se* did not alter the Barnes Maze assessment.

The link between stroke and dementia is poorly understood and has not been widely investigated. To the best of our knowledge, only one convincing study has addressed the relationships between sustained post-stroke inflammation and post-stroke dementia. C57Bl6J or BALBC/CJ mice were subjected to distal middle cerebral artery ligation and exhibited delayed cognitive decline seven weeks after stroke induction. Using an anti-CD20 antibody B-lymphocytes that had infiltrated the hippocampus were ablated, preventing thus cognitive deficit in these mice. T cells, MHCII expression, and markers of activated microglia/macrophages were also present in the brain at 12 weeks following stroke in the striatum and the internal capsule but their function was not specifically explored (Doyle et al., 2015). Interestingly, in patients who died with post-stroke dementia, post-mortem brain immunostaining also evidenced LB within and adjacent to the stroke core (Doyle et al., 2015). In our model, GA did not significantly modify learning but did preserve long-term memory. Vehicle-treated pMCAo diabetic mice took significantly longer to learn a new task than controls, whereas there were no differences between GA-treated mice and controls, suggesting that GA-treated mice learned the new task as quickly as controls. It is also possible that a longer treatment with GA (one month vs seven days) would have produced more striking effects, particularly in terms of learning abilities. Long term potentiation (LTP), a persistent increase in synaptic strength underlying the process of memory formation in the brain (Lynch, 2004), was shown to be impaired in stroke animals. Interestingly, Fingolimod,

an agonist of the sphingosine 1 phosphate receptor, which is thought to act through immunomodulation, prevents LTP impairment seven days post tMCAO in rats (Nazari et al., 2016). This finding together with our results on the memory-protective effects of GA after pMCAo highlight the potential of immunomodulators as a promising strategy to preserve memory function in the context of stroke. Nevertheless, diabetes *per se* enhances the risk of developing cognitive deficit (Schrijvers et al., 2010). Indeed, in addition to enhanced inflammation, cerebral hypoperfusion, impaired cerebral vasoreactivity (Last et al., 2007) and increased Aβ deposition in the brain (Saedi et al., 2016) likely also play a role.

Post-stroke dementia shares several common pathophysiological features with Alzheimer's disease (AD) including cerebral hypoperfusion, energy deficit, capillary dysfunction, inflammation, oxidative stress, and increased expression of Aβ and tau protein (Dong et al., 2018). Increased Aβ peptide levels are a hallmark of Alzheimer's dementia that likely contribute to memory impairment (Brito-Moreira et al., 2017). The distinct neurotoxicity of Aβ (Yankner and Lu, 2009) has also been identified in the ischemic brain (Dong et al., 2018). In a mouse model of AD (APPswe/PS1dE9 mice) subjected to tMCAo or photothrombosis-mediated microvessel occlusion, the transient increase in deposits of Aβ was evidenced in the whole brain and interpreted as an interference with amyloid clearance pathways (Garcia-Alloza et al., 2011). Several Aβ species are generated by proteolytic cleavage of amyloid precursor protein, ranging in length from 36 to 43 amino acids. The variants of 40 (Aβ40) and 42 (Aβ42) amino acids are the most abundant and when they adopt a β-sheet conformation they tend to aggregate to form insoluble neurotoxic deposits in the brain (Masters and Selkoe, 2012). It has been postulated that the shift of Aβ from a soluble to an insoluble form determines the severity of clinical dementia (Murphy et al., 2010; Wang et al., 1999). Interestingly, while highly amyloidogenic Aβ42 aggregates mainly within the cerebral parenchyma to form senile plaques, a defining diagnostic feature of AD (Selkoe and Hardy, 2016), Aβ40 has increased tropism for cerebral blood vessels where it aggregates leading to cerebral amyloid angiopathy (CAA) that is another prominent feature of AD (Grinberg et al., 2012). CAA is increasingly recognized as a major cause of cognitive impairment, similar to vascular cognitive impairment that may play an independent and potentiating role in Alzheimer's dementia (Banerjee et al., 2017). In this study, we demonstrate for the first time that cerebral ischemia results in significant accumulation of insoluble Aβ40 in the brain of diabetic mice six weeks after pMCAo, whereas pMCAo did not lead to aggregation of Aβ42, even though detectable amounts of soluble Aβ42 were found in the brains of operated animals. Importantly, while the soluble Aβ40 levels were significantly increased in GA-

treated mice, GA completely prevented the accumulation of insoluble Aβ40. Our results suggest that cerebral ischemia stimulates the generation of Aβ40 and its rapid conversion into insoluble aggregates, while GA inhibits the process of aggregation, likely by improving the scavenger function of microglia/macrophages and enhancing Aβ40 clearance from the brain. The enhanced the ability of macrophages cultured with GA to phagocytose preformed fibrillar amyloid-β1–42 has already been shown (Koronyo et al., 2015). These GA-treated macrophages exhibited increased expression of the scavenger receptors CD36 and SCARA1, which can facilitate amyloid-β phagocytosis. This may explain in part why some aspects of memory loss were prevented by GA in diabetic mice after pMCAo.

5. Conclusion

To the best of our knowledge, this is the first proof of concept study showing that in a context of exacerbated inflammation, GA may be effective in both the acute phase and in the long term in the cerebral ischemia setting. Other immunomodulatory therapies currently being evaluated have also shown promising results. INF-β, fingolimod (a sphingosine 1-phosphate receptor modulator), natalizumab (adhesion molecule inhibitor) and dimethyl fumarate provide functional recovery and/or reduce infarct volume (Dreikorn et al., 2018) depending on the animal species, stroke model (tMCAo vs pMCAo vs photothrombotic stroke vs intracerebral hemorrhage), therapeutic window, and dosage. These therapeutic approaches still require further investigation before being translated to the bedside (Kanazawa et al., 2015), particularly in view of the notable differences between the immune system in rodents and humans, such as the proportion of lymphocytes in the total leucocyte count (50–100% in rodents versus 20–40% in humans) (Sommer, 2017). Few phase 2 clinical trials on the efficacy of immune modulating therapies in stroke have been conducted: ACTION 2 (NCT02730455, completed, testing natalizumab), FAMTAIS (NCT02956200, on-going, testing fingolimod), FTY720 (NCT02002390, on-going, testing fingolimod) (clinicaltrials.org website). No clinical trials on glatiramer acetate have been reported to date. As already highlighted and as recommended by the Stroke Therapy Academic Industry Roundtable (STAIR) (Liu et al., 2009), our results should be replicated in other species, and the mechanisms further investigated. Immunomodulation is an emerging field of interest and nowadays one of the well-recognized mechanisms of action of stem cells/progenitor cells and mesenchymal cells in particular. Future clinical trials should explore the efficacy and safety of immunomodulators, either alone or in combination with mesenchymal stem cells.

Acknowledgements: This work was supported by INSERM, the French National Institute for Health and Medical Research; Gabrielle MANGIN received a grant from the RESSTORE project from H2020.

Disclosure of interest: The authors declare no conflicts of interest.

TABLES

Table 1. Primers used for real-time PCR. TNFα, tumor necrosis factor alpha; IL-1β, interleukin 1 beta ; IL-10, interleukin 10; TGFβ, transforming growth factor beta; IL-4, interleukin 4; CD206, cluster of differentiation 206; CD32, cluster of differentiation 32; CD86, cluster of differentiation 86; COX2, cyclooxygenase 2; Arg1, arginase1; CD68, cluster of differentiation 68; MCP1, monocyte chemoattractant protein 1; IL-6, interleukin 6.

Primer	Forward	Reverse
TNFα	TGGCCTCCCTCTCATCAGTTC	TTGGTGGTTTGCTACGACGTG
IL-1β	ACCTTCCAGGATGAGGACATGA	AACGTCACACACCAGCAGGTTA
IL-10	ACTGCACCCACTTCCCAGT	TGTCCAGCTGGTCCTTTGTT
TGFβ	TTGCTTCAGCTCCACAGAGA	TGGTTGTAGAGGGCAAGGAC
IL-4	TCAACCCCCAGCTAGTTGTC	TGTTCTTCGTTGCTGTGAGG
CD206	CTTCGGGCCTTT GGAATAAT	TAGAAGAGCCCTTGGGTTGA
CD32	CTGGAAGAAGCTGCCAAAAC	CCAATGCCAAGGGAGACTAA
CD86	CCAATGCCAAGGGAGACT AA	GGC TCT CAC TGC CTT CAC TC
COX2	TCATTCACCAGACAGATTGCT	AAGCGTTTGCGGTACTCATT
Arg1	GTGAAGAACCCACGGTCTGT	GCCAGAGATGCTTCCAACTG
CD68	TTCTGCTGTGGAAATGCAAG	AGAGGGGCTGGTAGGTTGAT
MCP1	AGGTCCCTGTCATGCTTCTG	TCTGGACCCATTCCTTCTTG
IL-6	AGTTGCCTTCTTGGGACTGA	TCCACGATTTCCCAGAGAAC

Table 2. Barnes maze assessment of latency to escape. C, control mice without diabetes or stroke; D, diabetic mice without stroke; Vehicle, diabetic mice with stroke treated with saline solution; GA, diabetic mice with stroke treated with GA; n, number of mice.

	C (n=10)	**D (n=7)**	**pMCAo (n=10)**	**Vehicle (n=17)**	**GA (n=16)**
1st day	165±50.56	183.20±54.57	150.40±31.89	184.1±59.03	168.40±57.79
2nd day	97.16±36.42	122.10±44.40	79.00±34.29	105.10±45.19	126.70±51.22
3rd day	59.13±21.02	82.32±41.65	47.13±25.85	85.48±24.04	103.00±60.74
4th day	41.58±11.93	42.08±28.00	34.94±13.56	65.29±37.77	70.781±39.68
7th day	38.43±20.41	28.75±11.58	28.55±13.66	72.35±38.90	32.99±15.52
8th day	47.27±16.08	68.76±32.47	52.57±25.17	121.50±42.12	96.56±41.23
9th day	37.33±14.45	39.23±20.17	29.27±12.95	97.35±70.08	46.59±21.10
10th day	34.00±27.50	36.05±13.36	31.70±22.61	84.05±61.68	46.44±26.85

Table 3. Normalized expression levels of mRNA encoding for pro- and anti-inflammatory mediators (a.u.) at one and seven days after permanent middle cerebral artery occlusion (pMCAo) in non-diabetic (C) and diabetic mice (D). IL-1β, interleukin-1 beta; MCP1, monocyte chemoattractant protein 1 ; CD68, cluster of differentiation 68 ; IL-6, interleukin 6; TNFα, tumor necrosis factor alpha; IL-4, interleukin 4. **P* < 0.05; ***P* < 0.01; ****P* < 0.001.

D1	**C + pMCAo**	**D + pMCAo**	***P* value**
IL-1β	0.11±0.06 (n=8)	1.71±1.79 (n=5)	0.025 *
MCP-1	1.15±0.58 (n=8)	3.36±2.66 (n=7)	0.038 *
CD68	1.13±0.29 (n=8)	0.93±0.16 (n=7)	0.12
IL-6	0.54±0.23 (n=7)	1.51±0.50 (n=6)	0.00076 ***
TNFα	3.18±1.41 (n=8)	10.72±5.76 (n=7)	0.0032 **
IL-4	1.14±0.61 (n=7)	1.03±0.22 (n=6)	0.87

D7	**C + pMCAo**	**D + pMCAo**	***P* value**
IL-1β	0.04±0.02 (n=6)	9.95±15.53 (n=7)	0.0032 **
MCP-1	0.18±0.05 (n=6)	1.56±1.53 (n=5)	0.050 *
CD68	0.56±0.53 (n=6)	1.81±0.79 (n=7)	0.027 *
IL-6	0.10±0.05 (n=5)	0.37±0.27 (n=5)	0.061
TNFα	0.40±0.31 (n=5)	3.31±2.31 (n=7)	0.0025 **
IL-4	0.55±0.32 (n=5)	0.099±0.079 (n=7)	0.0023 **

Table 4. Blood analysis for pro-inflammatory and anti-inflammatory cytokines at Day 3 and Day 40. TNFα, tumor necrosis factor alpha; IL-1β, interleukin 1 beta ; INFγ, Interferon gamma ; IL-4, interleukin 4 ; IL-10, interleukin 10 ; ND, not detected.

D3	Vehicle pg/ml (n=7)	GA (n=6) pg/ml	P value
TNFα	0.09263	0.03425	0.3320
IL-1β	ND	ND	/
INFγ	ND	ND	/
IL-4	0.00888	0.00850	0.9566
IL-10	0.000625	0.00025	0.2954

D40	Vehicle pg/ml (n=7)	GA pg/ml (n=6)	P value
TNFα	0.0296	0.06523	0.6958
IL-1β	ND	ND	/
INFγ	ND	ND	/
IL-4	0.01043	0.0106	0.9623
IL-10	ND	ND	/

Legends

Figure 1. A. Neurological score was significantly decreased at D1 after stroke induction in both GA and Vehicle mice (n=19-20, $P < 0.0001$****). **B.** At D3, a significant increase in the neurological score was detected in GA versus Vehicle mice (n=19-20, $P < 0.01$**) but not at D7 or D14. **C.** At D14, there were no significant differences in neurological scores compared to D-1 in the GA group, suggesting evidence of neurological recovery in contrast to the Vehicle group (n=16-19, $P < 0.01$**)**.**

Figure 2. A. Spontaneous activity of mice, assessed using the open-field test. No differences were observed between the three groups of diabetic mice in terms of the total distance traveled during the test or mean walking velocity. Only Control mice showed a significantly greater total distance traveled as well as mean walking velocity, compared to the three other groups (n=8-15, * $P < 0.05$, ** $P < 0.01$, *** $P < 0.001$). **B**. Learning capacity, long-term memory and new task learning were evaluated by the Barnes Maze test. The training phase showed that at D3, GA mice required significantly longer to learn the spatial navigation task (increased latency to escape) compared to pMCAo mice (n=10-17, GA vs pMCAo, $P < 0.05$*), but this was restored at D4 (n=10-17, $P > 0.05$). In the retention phase, only the Vehicle group showed impaired recall of the location of the escape box (n=7-17, § $P < 0.05$, §§ $P < 0.01$, §§§ $P < 0.001$), indicating that long-term memory was preserved in GA-treated mice. In the reversal phase, the Vehicle mice performed significantly less well than all the other groups except those treated with GA on the 8th day (C vs Vehicle, $P < 0.0001$ ****; D vs Vehicle, $P < 0.01$##; pMCAo vs Vehicle, $P < 0.0001$¤¤¤¤); GA-treated mice also performed less well than the C mice (P < 0.05 $). On the 9th and 10th days, the differences between the Vehicle mice and the other groups were seen to be the same (on the 9th day, C vs Vehicle, $P < 0.01$ **; D vs Vehicle, $P < 0.01$##; pMCAo vs Vehicle, $P < 0.001$¤¤¤; at the 10th, day, C vs Vehicle, $P < 0.05$ *; D vs Vehicle, $P < 0.05$#; pMCAo vs Vehicle, $P < 0.01$¤¤). On the 9th day, GA-treated mice performed significantly better than Vehicle mice ($P < 0.01$ &&).

Figure 3. Infarct volume was significantly reduced at D3 and D7 in GA mice (n=7, $P < 0,05$) (top, left), illustrated by Cresyl violet staining of coronal sections at D3 (right), whereas edema volume did not vary significantly regardless of whether the mice were treated with Vehicle or GA (bottom, left).

Figure 4. Microglia/macrophage cell density was not significantly modified by GA at D3 or D7 (n=7). Iba1 immunostaining in GA mice with magnification of resting form (top) and activated form (bottom) at D3 (left) and D7 (right). ROI, region of interest

Figure 5. A. At D3, COX2 mRNA levels were significantly decreased in GA mice compared to Vehicle mice ($P = 0.014$) whereas **CD32, TNFα, CD86 and IL-1β** mRNA levels were not affected by GA treatment. **B. At D7, COX2** mRNA levels were no longer significantly different between GA and Vehicle mice, whereas in contrast, **CD32**, **TNFα** and **IL-1β** mRNA levels were significantly decreased in GA-treated mice while **CD86** mRNA levels were not significantly different between groups (n=6-8, * $P < 0.05$, *** $P < 0.001$).

Figure 6. A. At D3, there were no significant differences in mRNA levels of chosen markers (**CD206**, **Arg1, IL-4**, **TGFβ** or **IL-10)** between the different groups. **B. At D7**, mRNA levels of these markers were still not significantly modified by GA with the exception of **IL-4** that was significantly increased in GA mice (n=5-8, $P < 0.01$**).

Figure 7. At D7, there was a significant increase in proliferating neuroblasts (KI67+/DCX+) in the GA mice compared to the Vehicle mice (n=5-7, $P < 0,05$*).

Figure 8. The distribution of Aβ40 between the soluble and insoluble pools was shifted by GA towards a soluble fraction. At D40, the Aβ42 soluble fraction was elevated in both GA- and Vehicle-treated groups and the insoluble fraction of Aβ42 was undetectable in both groups. In contrast, the Aβ40 soluble fraction was significantly increased in GA mice, whereas GA decreased the Aβ40 insoluble fraction dramatically and significantly to undetectable levels compared to Vehicle (n=8, ** $P < 0.01$, v $P < 0.001$).

REFERENCES

Banerjee G, Carare R, Cordonnier C, Greenberg SM, Schneider JA, Smith EE, Buchem MV, Grond JV, Verbeek MM, Werring DJ (2017) The increasing impact of cerebral amyloid angiopathy: essential new insights for clinical practice. Journal of neurology, neurosurgery, and psychiatry 88:982-994.

Benakis C, Garcia-Bonilla L, Iadecola C, Anrather J (2014) The role of microglia and myeloid immune cells in acute cerebral ischemia. Front Cell Neurosci 8:461.

Bhaskar S, Stanwell P, Cordato D, Attia J, Levi C (2018) Reperfusion therapy in acute ischemic stroke: dawn of a new era? BMC Neurol 18:8.

Brito-Moreira J, Lourenco MV, Oliveira MM, Ribeiro FC, Ledo JH, Diniz LP, Vital JFS, Magdesian MH, Melo HM, Barros-Aragao F, de Souza JM, Alves-Leon SV, Gomes FCA, Clarke JR, Figueiredo CP, De Felice FG, Ferreira ST (2017) Interaction of amyloid-beta (Abeta) oligomers with neurexin 2alpha and neuroligin 1 mediates synapse damage and memory loss in mice. The Journal of biological chemistry 292:7327-7337.

Burgess N, Maguire EA, O'Keefe J (2002) The human hippocampus and spatial and episodic memory. Neuron 35:625-641.

Chen R, Ovbiagele B, Feng W (2016) Diabetes and Stroke: Epidemiology, Pathophysiology, Pharmaceuticals and Outcomes. The American journal of the medical sciences 351:380-386.

Chhor V, Le Charpentier T, Lebon S, Ore MV, Celador IL, Josserand J, Degos V, Jacotot E, Hagberg H, Savman K, Mallard C, Gressens P, Fleiss B (2013) Characterization of phenotype markers and neuronotoxic potential of polarised primary microglia in vitro. Brain Behav Immun 32:70-85.

Cifuentes D, Poittevin M, Bonnin P, Ngkelo A, Kubis N, Merkulova-Rainon T, Levy BI (2017) Inactivation of Nitric Oxide Synthesis Exacerbates the Development of Alzheimer Disease Pathology in APPPS1 Mice (Amyloid Precursor Protein/Presenilin-1). Hypertension 70:613-623.

Cruz Y, Lorea J, Mestre H, Kim-Lee JH, Herrera J, Mellado R, Gálvez V, Cuellar L, Musri C, Ibarra A (2015) Copolymer-1 promotes neurogenesis and improves functional recovery after acute ischemic stroke in rats. PloS one 10:e0121854.

Dave KR, Tamariz J, Desai KM, Brand FJ, Liu A, Saul I, Bhattacharya SK, Pileggi A (2011) Recurrent hypoglycemia exacerbates cerebral ischemic damage in streptozotocin-induced diabetic rats. Stroke 42:1404-1411.

Dinel AL, Andre C, Aubert A, Ferreira G, Laye S, Castanon N (2011) Cognitive and emotional alterations are related to hippocampal inflammation in a mouse model of metabolic syndrome. PLoS One 6:e24325.

Dong S, Maniar S, Manole MD, Sun D (2018) Cerebral Hypoperfusion and Other Shared Brain Pathologies in Ischemic Stroke and Alzheimer's Disease. Translational stroke research 9:238-250.

Doyle KP, Quach LN, Sole M, Axtell RC, Nguyen TV, Soler-Llavina GJ, Jurado S, Han J, Steinman L, Longo FM, Schneider JA, Malenka RC, Buckwalter MS (2015) B-lymphocyte-mediated delayed cognitive impairment following stroke. J Neurosci 35:2133-2145.

Dreikorn M, Milacic Z, Pavlovic V, Meuth SG, Kleinschnitz C, Kraft P (2018) Immunotherapy of experimental and human stroke with agents approved for multiple sclerosis: a systematic review. Therapeutic advances in neurological disorders 11:1756286418770626.

Ekdahl CT, Kokaia Z, Lindvall O (2009) Brain inflammation and adult neurogenesis: the dual role of microglia. Neuroscience 158:1021-1029.

Franco R, Fernandez-Suarez D (2015) Alternatively activated microglia and macrophages in the central nervous system. Progress in neurobiology 131:65-86.

Fumagalli S, Perego C, Pischiutta F, Zanier ER, De Simoni MG (2015) The ischemic environment drives microglia and macrophage function. Front Neurol 6:81.

Garcia-Alloza M, Gregory J, Kuchibhotla KV, Fine S, Wei Y, Ayata C, Frosch MP, Greenberg SM, Bacskai BJ (2011) Cerebrovascular lesions induce transient beta-amyloid deposition. Brain : a journal of neurology 134:3697-3707.

Gelderblom M, Leypoldt F, Steinbach K, Behrens D, Choe CU, Siler DA, Arumugam TV, Orthey E, Gerloff C, Tolosa E, Magnus T (2009) Temporal and spatial dynamics of cerebral immune cell accumulation in stroke. Stroke 40:1849-1857.

Gorelick PB, Scuteri A, Black SE, Decarli C, Greenberg SM, Iadecola C, Launer LJ, Laurent S, Lopez OL, Nyenhuis D, Petersen RC, Schneider JA, Tzourio C, Arnett DK, Bennett DA, Chui HC, Higashida RT, Lindquist R, Nilsson PM, Roman GC, Sellke FW, Seshadri S, American Heart Association Stroke Council CoE, Prevention CoCNCoCR, Intervention, Council on Cardiovascular S, Anesthesia (2011) Vascular contributions to cognitive impairment and dementia: a statement for healthcare professionals from the american heart association/american stroke association. Stroke 42:2672-2713.

Grinberg LT, Korczyn AD, Heinsen H (2012) Cerebral amyloid angiopathy impact on endothelium. Experimental gerontology 47:838-842.

Gronberg NV, Johansen FF, Kristiansen U, Hasseldam H (2013) Leukocyte infiltration in experimental stroke. Journal of neuroinflammation 10:115.

Haddad M, Beray-Berthat V, Coqueran B, Palmier B, Szabo C, Plotkine M, Margaill I (2008) Reduction of hemorrhagic transformation by PJ34, a poly(ADP-ribose)polymerase inhibitor, after permanent focal cerebral ischemia in mice. European journal of pharmacology 588:52-57.

Harrison FE, Hosseini AH, McDonald MP (2009) Endogenous anxiety and stress responses in water maze and Barnes maze spatial memory tasks. Behavioural brain research 198:247-251.

Hu X, Li P, Guo Y, Wang H, Leak RK, Chen S, Gao Y, Chen J (2012) Microglia/macrophage polarization dynamics reveal novel mechanism of injury expansion after focal cerebral ischemia. Stroke; a Journal of Cerebral Circulation 43:3063-3070.

Hwang IK, Choi JH, Nam SM, Park OK, Yoo DY, Kim W, Yi SS, Won MH, Seong JK, Yoon YS (2014) Activation of microglia and induction of pro-inflammatory cytokines in the hippocampus of type 2 diabetic rats. Neurological research 36:824-832.

Ibarra A, Avendaño H, Cruz Y (2007) Copolymer-1 (Cop-1) improves neurological recovery after middle cerebral artery occlusion in rats. Neuroscience letters 425:110-113.

Jones KA, Maltby S, Plank MW, Kluge M, Nilsson M, Foster PS, Walker FR (2018) Peripheral immune cells infiltrate into sites of secondary neurodegeneration after ischemic stroke. Brain, behavior, and immunity 67:299-307.

Jovin TG, Chamorro A, Cobo E, de Miquel MA, Molina CA, Rovira A, San Roman L, Serena J, Abilleira S, Ribo M, Millan M, Urra X, Cardona P, Lopez-Cancio E, Tomasello A, Castano C, Blasco J, Aja L, Dorado L, Quesada H, Rubiera M, Hernandez-Perez M, Goyal M, Demchuk AM, von Kummer R, Gallofre M, Davalos A, Investigators RT (2015) Thrombectomy within 8 hours after symptom onset in ischemic stroke. N Engl J Med 372:2296-2306.

Kanazawa M, Kawamura K, Takahashi T, Miura M, Tanaka Y, Koyama M, Toriyabe M, Igarashi H, Nakada T, Nishihara M, Nishizawa M, Shimohata T (2015) Multiple therapeutic effects of progranulin on experimental acute ischaemic stroke. Brain 138:1932-1948.

Kanazawa M, Ninomiya I, Hatakeyama M, Takahashi T, Shimohata T (2017) Microglia and Monocytes/Macrophages Polarization Reveal Novel Therapeutic Mechanism against Stroke. International journal of molecular sciences 18.

Koronyo Y, Salumbides BC, Sheyn J, Pelissier L, Li S, Ljubimov V, Moyseyev M, Daley D, Fuchs DT, Pham M, Black KL, Rentsendorj A, Koronyo-Hamaoui M (2015) Therapeutic effects of glatiramer acetate and grafted CD115(+) monocytes in a mouse model of Alzheimer's disease. Brain : a journal of neurology 138:2399-2422.

Kraft P, Göbel K, Meuth SG, Kleinschnitz C (2014) Glatiramer acetate does not protect from acute ischemic stroke in mice. Experimental & translational stroke medicine 6:4.

Kubis N (2016) Non-Invasive Brain Stimulation to Enhance Post-Stroke Recovery. Frontiers in neural circuits 10:56.

Last D, Alsop DC, Abduljalil AM, Marquis RP, de Bazelaire C, Hu K, Cavallerano J, Novak V (2007) Global and regional effects of type 2 diabetes on brain tissue volumes and cerebral vasoreactivity. Diabetes care 30:1193-1199.
Lehmann J, Hartig W, Seidel A, Fuldner C, Hobohm C, Grosche J, Krueger M, Michalski D (2014) Inflammatory cell recruitment after experimental thromboembolic stroke in rats. Neuroscience 279:139-154.
Liesz A, Hu X, Kleinschnitz C, Offner H (2015) Functional role of regulatory lymphocytes in stroke: facts and controversies. Stroke 46:1422-1430.
Liu S, Zhen G, Meloni BP, Campbell K, Winn HR (2009) RODENT STROKE MODEL GUIDELINES FOR PRECLINICAL STROKE TRIALS (1ST EDITION). Journal of experimental stroke & translational medicine 2:2-27.
Lynch MA (2004) Long-term potentiation and memory. Physiological reviews 84:87-136.
Makinen S, van Groen T, Clarke J, Thornell A, Corbett D, Hiltunen M, Soininen H, Jolkkonen J (2008) Coaccumulation of calcium and beta-amyloid in the thalamus after transient middle cerebral artery occlusion in rats. J Cereb Blood Flow Metab 28:263-268.
Masters CL, Selkoe DJ (2012) Biochemistry of amyloid beta-protein and amyloid deposits in Alzheimer disease. Cold Spring Harb Perspect Med 2:a006262.
McBride DW, Zhang JH (2017) Precision Stroke Animal Models: the Permanent MCAO Model Should Be the Primary Model, Not Transient MCAO. Translational stroke research.
Murphy MP, LeVine H, 3rd. Alzheimer's disease and the amyloid-beta peptide. Journal of Alzheimer's disease : JAD. 2010;19(1):311-23.
Nazari M, Keshavarz S, Rafati A, Namavar MR, Haghani M (2016) Fingolimod (FTY720) improves hippocampal synaptic plasticity and memory deficit in rats following focal cerebral ischemia. Brain research bulletin 124:95-102.
Organization WH WHO | The top 10 causes of death. In: WHO.
Ozen I, Deierborg T, Miharada K, Padel T, Englund E, Genove G, Paul G (2014) Brain pericytes acquire a microglial phenotype after stroke. Acta neuropathologica 128:381-396.
Planas AM, Gorina R, Chamorro A (2006) Signalling pathways mediating inflammatory responses in brain ischaemia. Biochem Soc Trans 34:1267-1270.
Poittevin M, Bonnin P, Pimpie C, Rivière L, Sebrié C, Dohan A, Pocard M, Charriaut-Marlangue C, Kubis N (2015) Diabetic microangiopathy: impact of impaired cerebral vasoreactivity and delayed angiogenesis after permanent middle cerebral artery occlusion on stroke damage and cerebral repair in mice. Diabetes 64:999-1010.
Poittevin M, Deroide N, Azibani F, Delcayre C, Giannesini C, Levy BI, Pocard M, Kubis N (2013) Glatiramer Acetate administration does not reduce damage after cerebral ischemia in mice. Journal of neuroimmunology 254:55-62.
Roychaudhuri R, Yang M, Hoshi MM, Teplow DB (2009) Amyloid beta-protein assembly and Alzheimer disease. J Biol Chem 284:4749-4753.
Saedi E, Gheini MR, Faiz F, Arami MA (2016) Diabetes mellitus and cognitive impairments. World journal of diabetes 7:412-422.
Schrijvers EM, Witteman JC, Sijbrands EJ, Hofman A, Koudstaal PJ, Breteler MM (2010) Insulin metabolism and the risk of Alzheimer disease: the Rotterdam Study. Neurology 75:1982-1987.
Selkoe DJ, Hardy J (2016) The amyloid hypothesis of Alzheimer's disease at 25 years. EMBO molecular medicine 8:595-608.
Snyder HM, Corriveau RA, Craft S, Faber JE, Greenberg SM, Knopman D, Lamb BT, Montine TJ, Nedergaard M, Schaffer CB, Schneider JA, Wellington C, Wilcock DM, Zipfel GJ, Zlokovic B, Bain LJ, Bosetti F, Galis ZS, Koroshetz W, Carrillo MC (2015) Vascular contributions to cognitive impairment and dementia including Alzheimer's disease. Alzheimer's & dementia : the journal of the Alzheimer's Association 11:710-717.
Sommer CJ. Ischemic stroke: experimental models and reality. Acta Neuropathol. 2017;133(2):245-261.

Srikanth VK, Thrift AG, Saling MM, Anderson JF, Dewey HM, Macdonell RA, Donnan GA, Community-Based Prospective Study of Nonaphasic English-Speaking S (2003) Increased risk of cognitive impairment 3 months after mild to moderate first-ever stroke: a Community-Based Prospective Study of Nonaphasic English-Speaking Survivors. Stroke 34:1136-1143.

Stein M, Keshav S, Harris N, Gordon S (1992) Interleukin 4 potently enhances murine macrophage mannose receptor activity: a marker of alternative immunologic macrophage activation. J Exp Med 176:287-292.

Tong HV, Luu NK, Son HA, Hoan NV, Hung TT, Velavan TP, Toan NL (2017) Adiponectin and pro-inflammatory cytokines are modulated in Vietnamese patients with type 2 diabetes mellitus. Journal of diabetes investigation 8:295-305.

Tureyen K, Bowen K, Liang J, Dempsey RJ, Vemuganti R (2011) Exacerbated brain damage, edema and inflammation in type-2 diabetic mice subjected to focal ischemia. J Neurochem 116:499-507.

van Groen T, Puurunen K, Maki HM, Sivenius J, Jolkkonen J (2005) Transformation of diffuse beta-amyloid precursor protein and beta-amyloid deposits to plaques in the thalamus after transient occlusion of the middle cerebral artery in rats. Stroke 36:1551-1556.

Wang J, Dickson DW, Trojanowski JQ, Lee VM. The levels of soluble versus insoluble brain Abeta distinguish Alzheimer's disease from normal and pathologic aging. Experimental neurology. 1999;158(2):328-37.

Whishaw IQ (1995) A comparison of rats and mice in a swimming pool place task and matching to place task: some surprising differences. Physiol Behav 58:687-693.

Yankner BA, Lu T (2009) Amyloid beta-protein toxicity and the pathogenesis of Alzheimer disease. The Journal of biological chemistry 284:4755-4759.

Zhang J, Zhang Y, Xing S, Liang Z, Zeng J (2012) Secondary neurodegeneration in remote regions after focal cerebral infarction: a new target for stroke management? Stroke 43:1700-1705.

Zhou W, Liesz A, Bauer H, Sommer C, Lahrmann B, Valous N, Grabe N, Veltkamp R (2013) Postischemic Brain Infiltration of Leukocyte Subpopulations Differs among Murine Permanent and Transient Focal Cerebral Ischemia Models. Brain Pathology 23:34–44.

Figure 1. Assessment of sensorimotor deficit

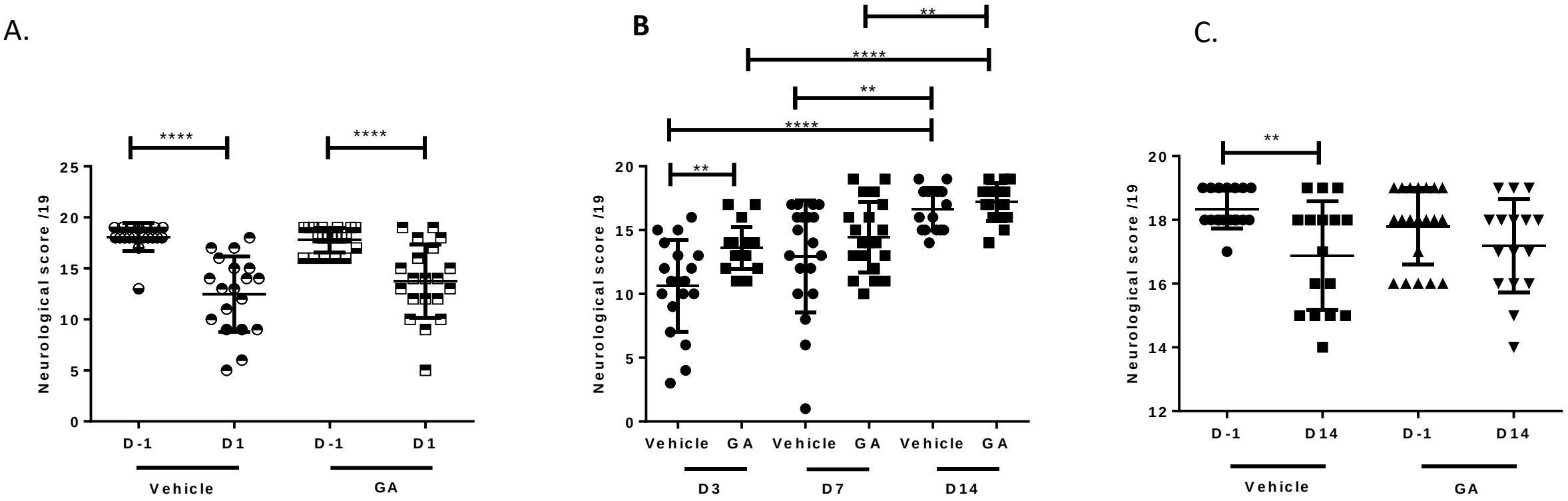

Figure 2. Assessment of cognitive decline

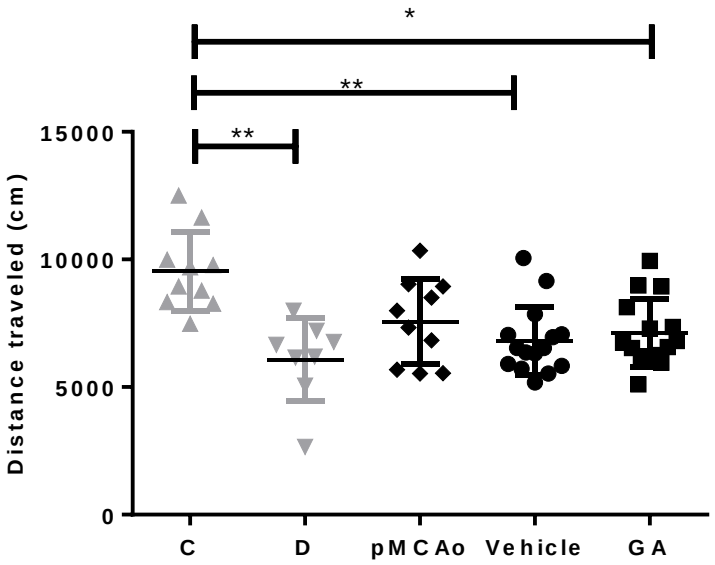

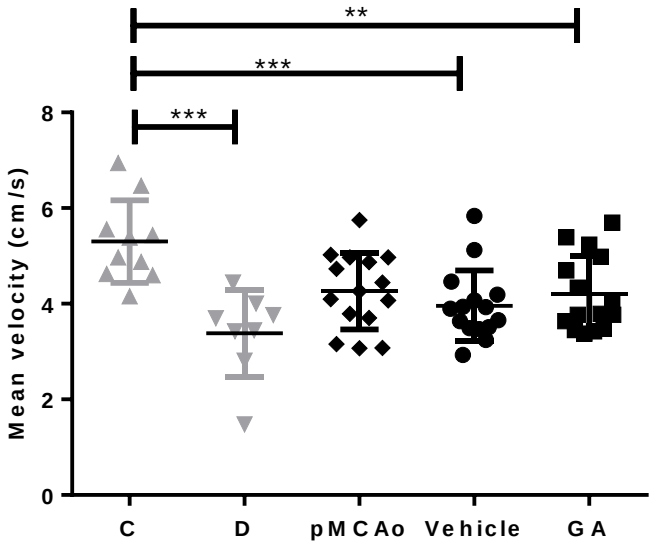

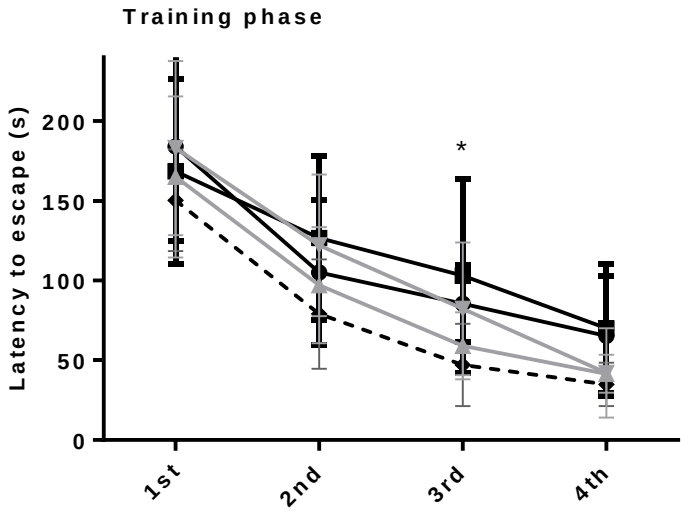

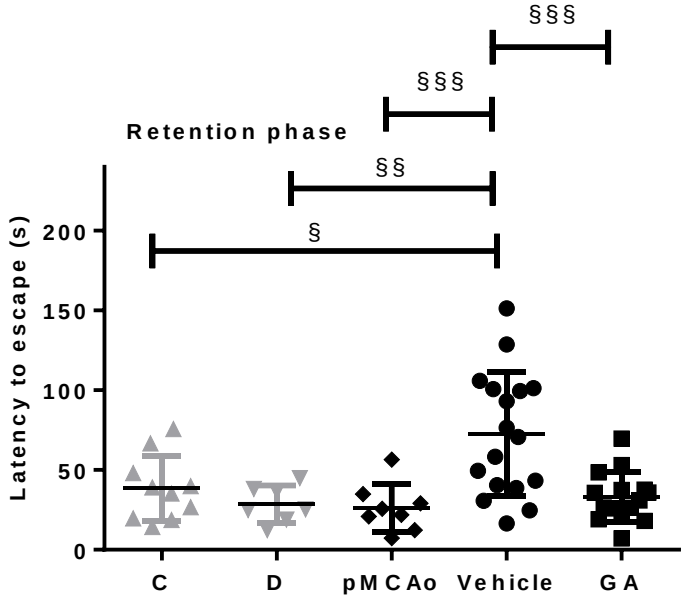

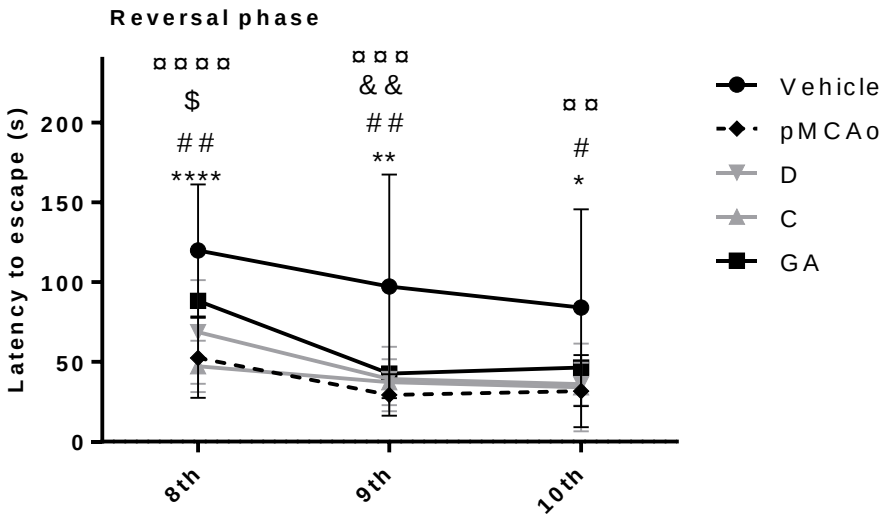

Figure 3. Stroke volume and edema

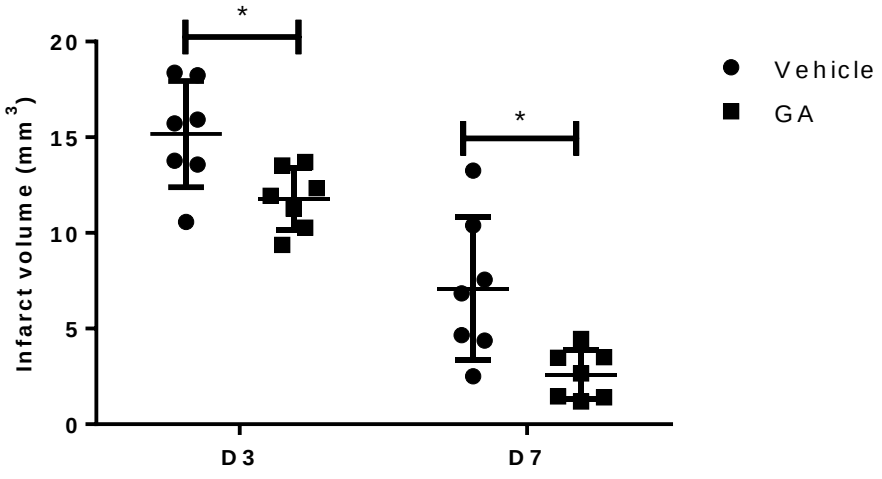

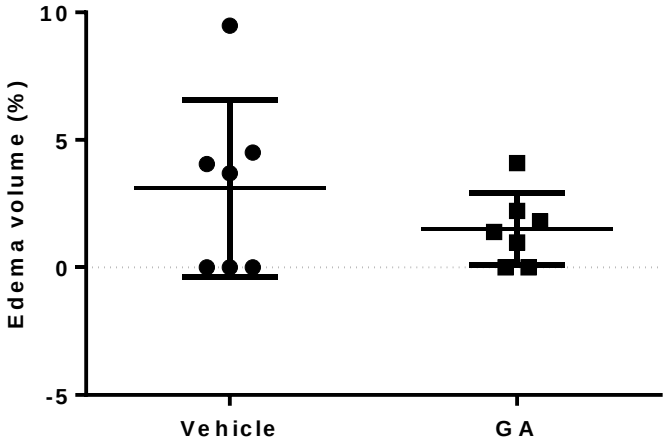

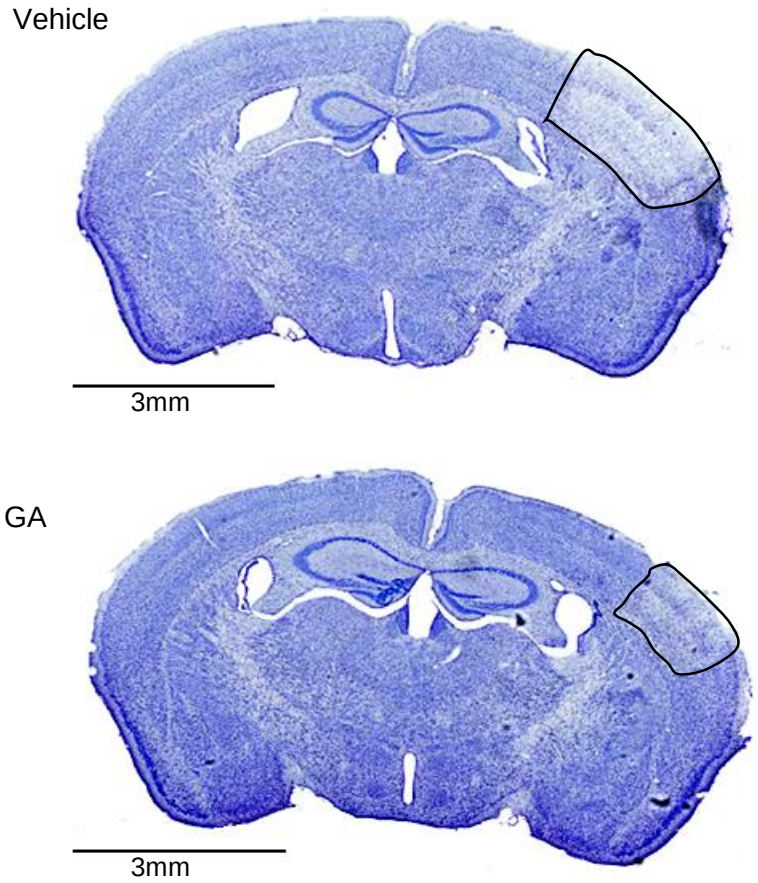

Figure 4. Microglia/macrophage cell density

D3

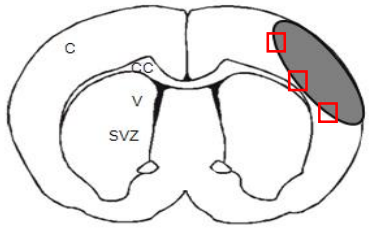

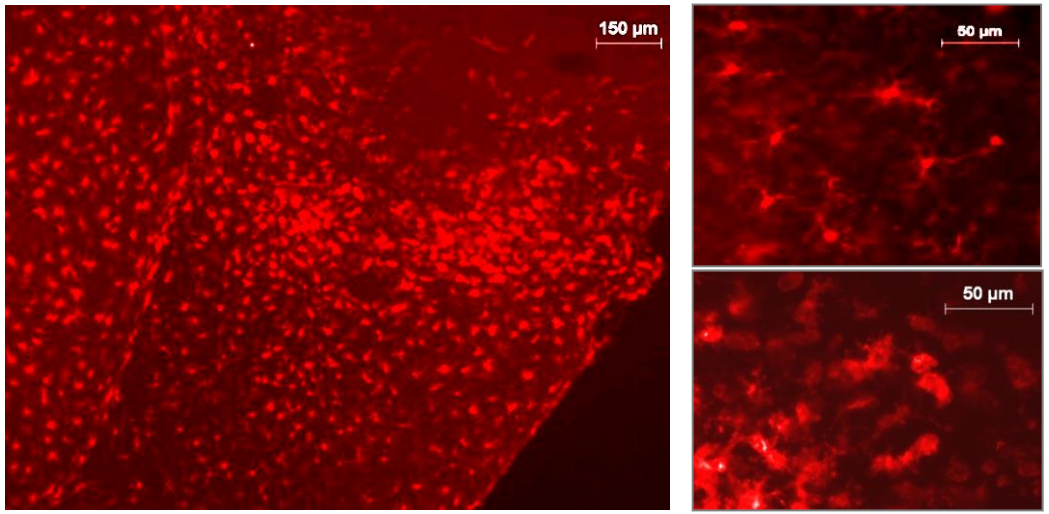

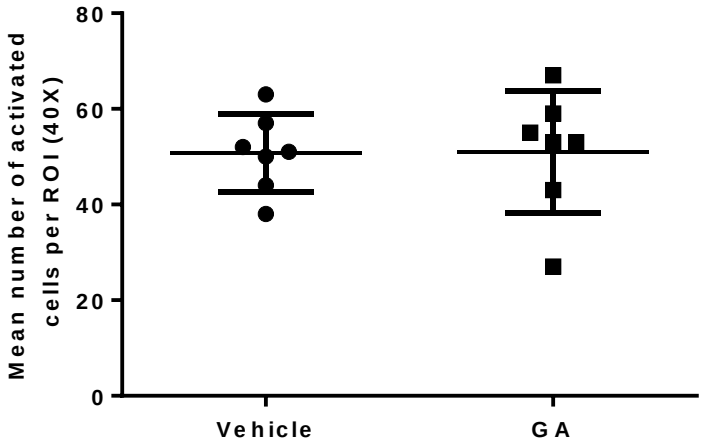

D7

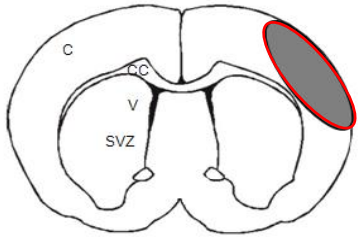

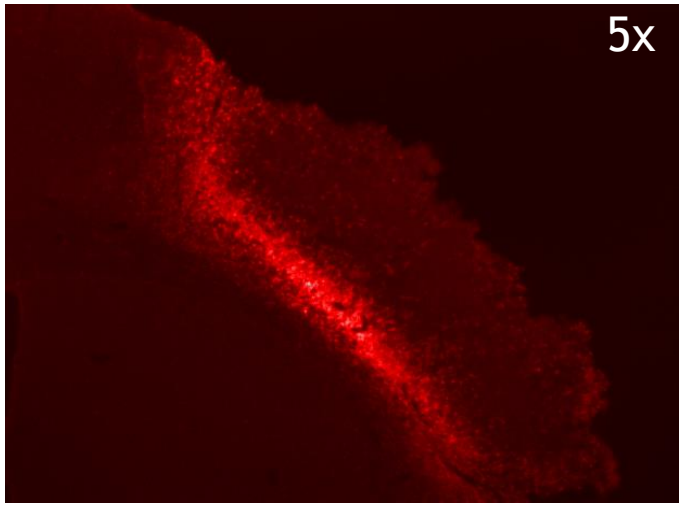

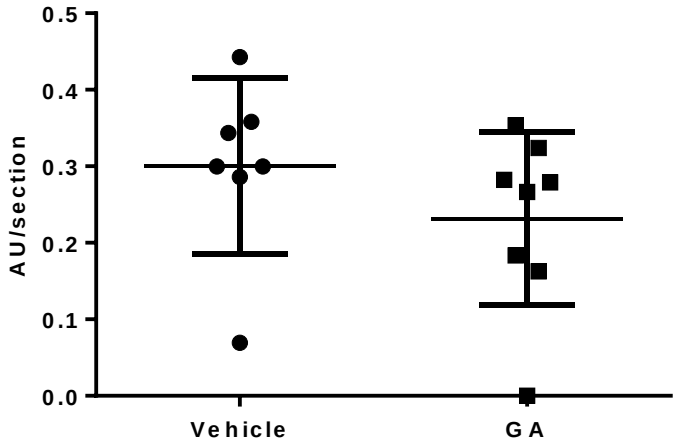

Figure 5. Expression of proinflammatory mediators at D3 and D7

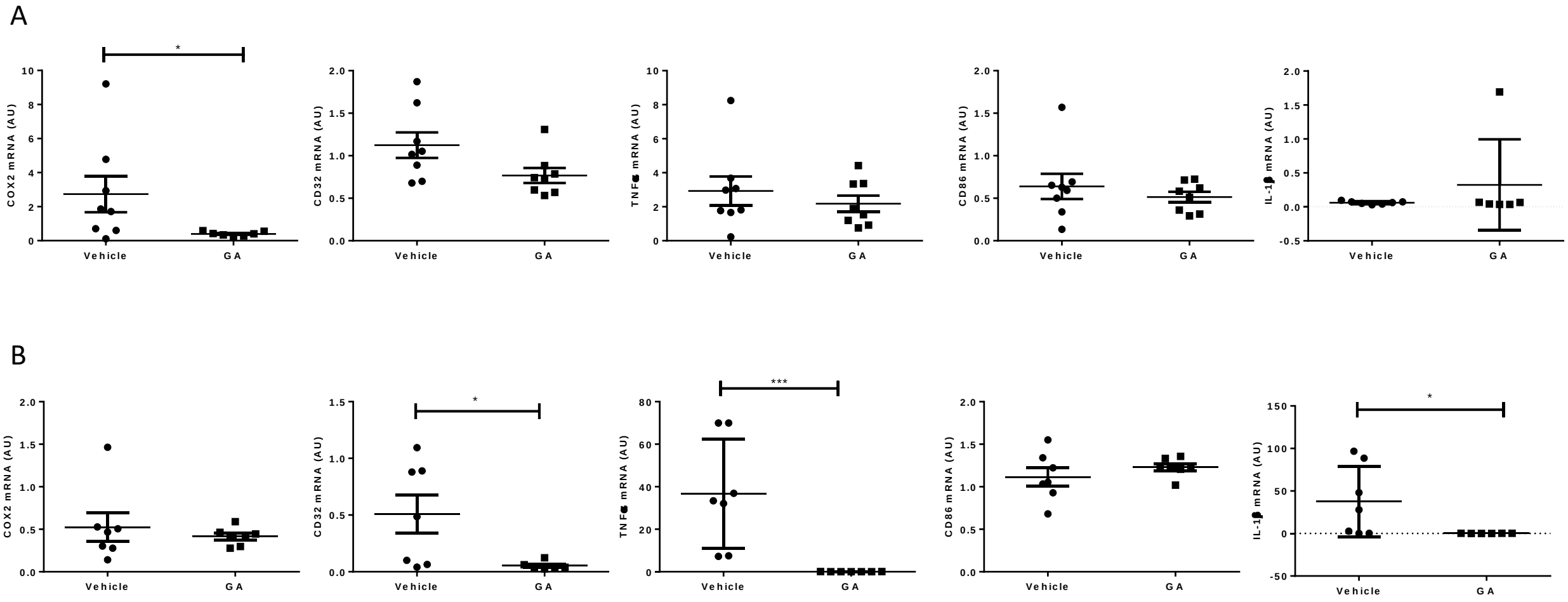

Figure 6. Expression of anti-inflammatory mediators at D3 and at D7

A

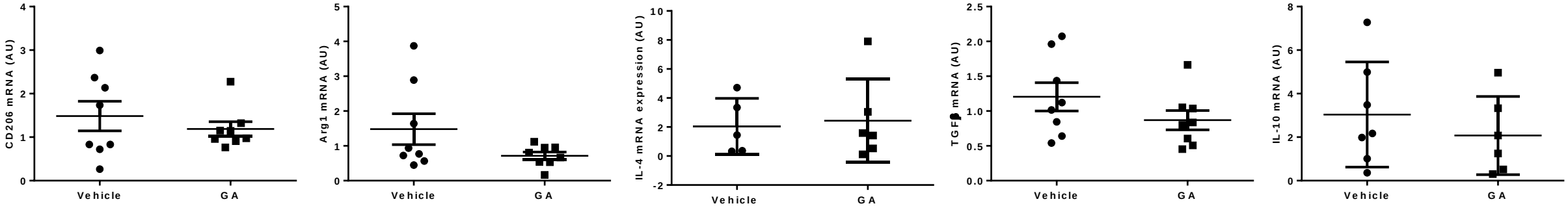

B

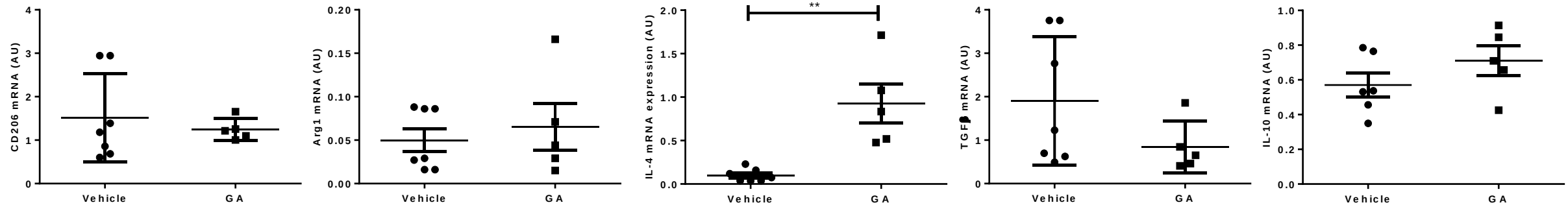

Figure 7. Neurogenesis at D7

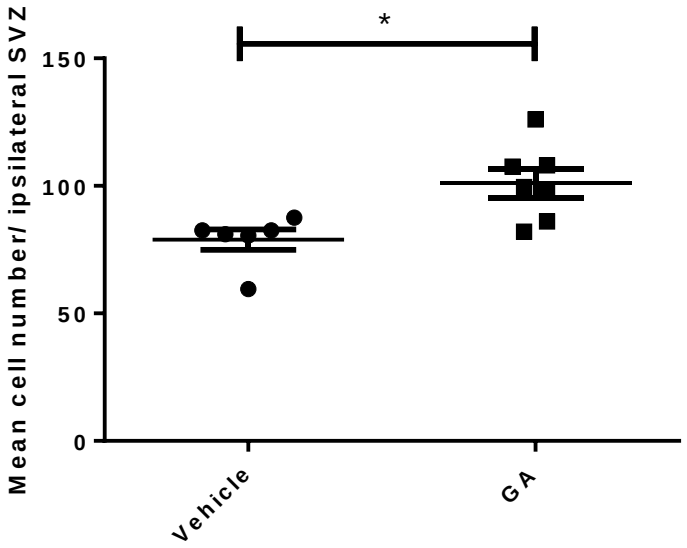

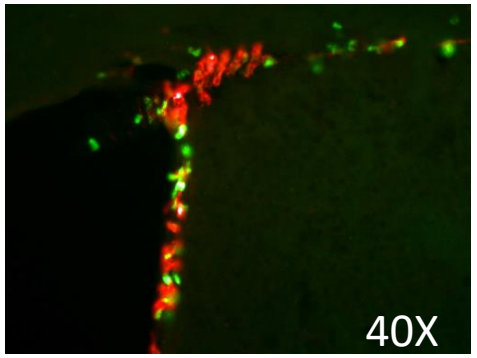

Vehicle

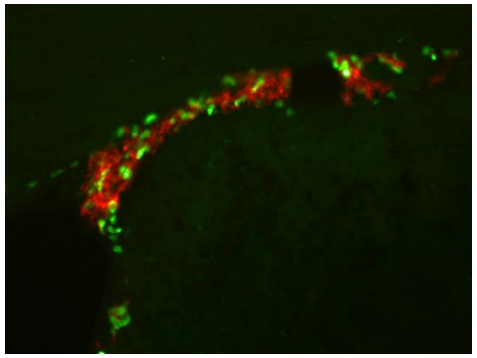

GA

Figure 8. Distribution of Aβ40 and Aβ42